# Synthetic and Mechanistic Pathways of *Cis* and *Trans*-Hydroxytamoxifen Drug Derivatives Reacting with Cp*Rh Complexes that involve $\eta^1$-N, $\eta^2$-N,O, $\eta^1$-O, and $\eta^6$ Bonding Modes, via a Novel N-$\pi$ Rearrangement; Relative Binding Affinities and Computer Docking Studies of *Cis and Trans*-$\eta^6$-Cp*Rh-Hydroxytamoxifen Complexes at the Estrogen, ER$\alpha$ and ER$\beta$ Receptors, and Growth Inhibition to Breast Cancer Cells

Siden Top,[†] Irena Efremenko,[‡] Marie Noelle Rager,[§] Anne Vessières,[†] Paul Yaswen,[||] Gérard Jaouen,[†] and Richard H. Fish*,[||]

[†]*Ecole Nationale Supérieure de Chimie de Paris, Laboratoire Charles Friedel, UMR 7223, 11, rue Pierre et Marie Curie, F-75231 Paris Cedex 05, France,* [‡]*Department of Organic Chemistry, Weizmann Institute of Science, Rehovot 76100, Israel,* [§]*Laboratoire de RMN, Ecole Nationale Supérieure De Chimie de Paris, 11 rue Pierre et Marie Curie, F 75213 Paris Cedex 05, France, and* [||]*Lawrence Berkeley National Laboratory, University of California, Berkeley, California 94720, United States*

The reactions of the breast cancer drug metabolite derivatives of tamoxifen, *cis* and *trans*-hydroxytamoxifen, **cis-1** and **trans-2**, with [Cp*Rh(L)$_3$]$^{2+}$ complexes (L = H$_2$O or MeOH), in CH$_2$Cl$_2$ and CH$_3$OH solvents, initially provided the kinetic $\eta^1$-N complexes, **cis-4** (OTf $^-$, **CH$_3$OH**) and **trans-5** (OTf $^-$, **CH$_3$OH**), which underwent a novel, regioselective, intramolecular N-$\pi$ rearrangement to give the *cis* and *trans*-$\eta^6$-phenol substituted complexes, **cis-6** and **trans-7**, via $\eta^2$-N,O, $\eta^1$-O, and ether aromatic ring $\eta^6$ intermediates. Recent density functional theory (DFT) calculations showed a preferred ground state for $\eta^1$-N; $\eta^2$-N,O; $\eta^1$-O; and the $\eta^6$ complexes, including the prominent roles of the triflate anion (OTf $^-$), and solvent molecules (CH$_2$Cl$_2$ and CH$_3$OH), and provided further steric, electronic, and thermodynamic data on the mechanism of the N-$\pi$ rearrangement. The $\eta^6$ complex, **cis-6**, was shown to be an antagonist for ER$\alpha$ estrogen receptor binding, in a competition experiment with the female hormone, estradiol; therefore, computer docking studies of this biologically active complex at the estrogen receptors, ER$\alpha$ and ER$\beta$, also provided information on the binding modes and thermodynamic parameters, while bioassay results provided growth inhibition data on both hormone dependent and independent breast cancer cell lines.

## Introduction

The study of organometallic pharmaceuticals has been shown to be a viable discipline for new drug discovery, as well as their potential utilization for disease therapy.[1] Moreover, it has been demonstrated that the modification of the structures of known drugs; for example, the *cis* and *trans* isomer metabolite derivatives of the breast cancer drug, tamoxifen, **cis-1** and **trans-2**, with a ferrocenyl moiety, in place of a phenyl group, ferrocifen, **3**, provided an antagonist compound, which was found to bind at the estrogen receptor, in competition with the female hormone, estradiol.[1g,h,2] Complex **3** also demonstrated an enhanced growth inhibition effect, for a potential, future therapy for breast cancer, as well as a variety of other cancers.[1k,2]

Therefore, there were several important reasons for further studying the hydroxytamoxifen derivatives, **cis-1** and **trans-2**, with a three spacer methylene, instead of the

*To whom correspondence should be addressed. E-mail: rhfish@lbl.gov.
(1) (a) Fish, R. H.; Jaouen, G. *Organometallics* **2003**, *22*, 2166, and references therein. (b) Allardyce, C. S.; Dyson, P. J.; Ellis, D. J.; Heath, S. L. *Chem. Commun.* **2001**, 1396. (c) Allardyce, C. S.; Dyson, P. J.; Ellis, D. J.; Salter, P. A.; Scopelliti, R. *J. Organomet. Chem.* **2003**, *668*, 35. (d) Morris, R. E.; Aird, R. E.; Murdoch, P. D.; Chen, H. M.; Cummings, J.; Hughes, N. D.; Parsons, S.; Parkin, A.; Boyd, G.; Jodrell, G. D. I.; Sadler, P. J. *J. Med. Chem.* **2001**, *44*, 3621. (e) Chen, H.; Parkinson, J. A.; Parsons, S.; Coxall, R. A.; Gould, R. O.; Sadler, P. J. *J. Am. Chem. Soc.* **2002**, *124*, 3064. (f) Wang, F.; Chen, H.; Parkinson, J. A.; Murdoch, P. D.; Sadler, P. J. *Inorg. Chem.* **2002**, *41*, 4509. (g) Jaouen, G.; Top, S.; Vessières, A.; Alberto, R. *J. Organomet. Chem.* **2000**, *600*, 25, and references therein. (h) Jaouen, G. *Chem. Br.* **2001**, 36. (i) Köpf-Maier, P. *Eur. J. Chim. Pharmacol.* **1994**, *47*, 1. (j) Melchart, M.; Sadler, P. J. In *Bioorganometallics*; Jaouen, G., Ed.; Wiley-VCH: Weinheim, Germany, 2005; Chapter 2, p 39. (k) Jaouen, G.; Top, S.; Vessières, A. In *Bioorganometallics*; Jaouen, G., Ed.; Wiley-VCH: Weinheim, Germany, 2005; Chapter 3, p 65. (l) Alberto, R. In *Bioorganometallics*; Jaouen, G., Ed.; Wiley-VCH: Weinheim, Germany, 2005; Chapter 4, p 97. (m) Dagani, R. *Chem. Eng. News* **2002**, *80*, 23; September 16, 2002 issue. "The Bio Side of Organometallics." (n) Dorcier, A.; Hartinger, C. G.; Scopelliti, R.; Fish, R. H.; Keppler, B. K.; Dyson, P. J. *J. Inorg. Biochem.* **2008**, *102*, 1066. (o) Peacock, A. F. A.; Sadler, P. J. *Chem. Asian J.* **2008**, *11*, 1886. (p) Hartinger, C. G.; Dyson, P. J. *Chem. Soc. Rev.* **2009**, *38*, 391. (q) Strohfeldt, K.; Tacke, M. *Chem. Soc. Rev.* **2008**, *37*, 1174.

(2) (a) Top, S.; Vessières, A.; Leclercq, G.; Quivy, J.; Tang, J.; Vaissermann, J.; Huché, M.; Jaouen, G. *Chem.—Eur. J.* **2003**, *9*, 5223. (b) El Amouri, H.; Vessières, A.; Vichard, D.; Top, S.; Gruselle, M.; Jaouen, G. *J. Med. Chem.* **1992**, *35*, 3130. (c) Jaouen, G.; Top, S.; Vessières, A.; Leclercq, G.; Quivy, J.; Jin, L.; Croisy, A. *C. R. Acad. Sci., Paris* **2000**, *3*, 89.

two spacer methylene utilized in the actual tamoxifen breast cancer drug, and were predicated on previous bioassay studies on complex **3**, where maximum bioactivity was achieved with the three methylene tether, and the hydroxylation of one of the phenyl groups; in the actual tamoxifen drug given to women, the P450 liver enzymes metabolized and activated the drug to provide the essential phenol substituent, in vivo.[2]



*cis*-**1**  *trans*-**2**

**3**  *cis*-**tamoxifen**
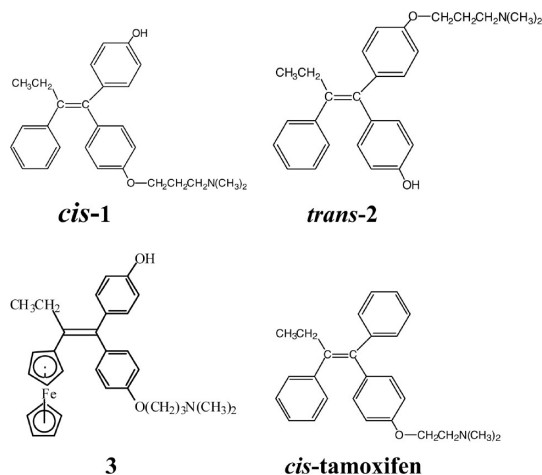
Furthermore, our continuing interest involving the bioorganometallic chemistry of organorhodium complexes[1a,3] led to new approaches for a strategy on further modifying the basic structure of **cis**-**1** and **trans**-**2**; as far as we are aware, our initial report on the synthesis of organorhodium complexes of the tamoxifen drug derivatives, **cis**-**1** and **trans**-**2**, was the first for this potential class of organometallic pharmaceutical breast cancer drugs.[4] More importantly, in that initial communication,[4] we discovered a novel, regioselective, intramolecular N-$\pi$ rearrangement that provided water-soluble *cis* and *trans*-$\eta^6$-Cp*Rh-hydroxytamoxifen complexes, which we now report that the *cis*-$\eta^6$ complex, **cis**-**6**, was found to inhibit the growth of several breast cancer cell lines, as well as being a potential probe for more information concerning its computer docking studies, including van der Waal/electrostatic interactions at the isoforms of the estrogen receptors, ER$\alpha$ and ER$\beta$. In this contribution, we report the full details on the synthesis, mechanism of the N-$\pi$ rearrangement, and biological aspects of the *cis* and *trans*-$\eta^6$-Cp*Rh-hydroxytamoxifen complexes.

## Results and Discussion

**Synthesis of Cp*Rh-Hydroxytamoxifen Complexes.** The previously reported synthesis of the tamoxifen derivatives, **cis**-**1** and **trans**-**2**, by Top et al., is shown in eq 1.[5]



(1)
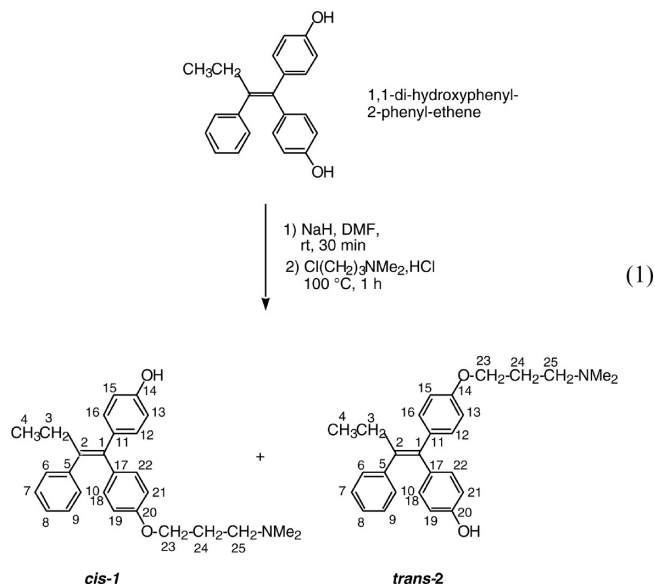
Thus, the synthetic strategy we followed was dictated by the lack of solubility of **cis**-**1** or **trans**-**2** in water, including their ammonium salt derivatives. Therefore, we initially studied, via ^{1}H NMR spectroscopy, the reactions of in situ formed [Cp*Rh(CH_3OH-d_4)_3](OTf)_2 with **cis**-**1** or **trans**-**2** at room temperature (RT), in CD_3OD-d_4. This afforded interesting results, in that the initial kinetically controlled product, from each individual **cis**-**1** or **trans**-**2** compound, was the $\eta^1$-N-Cp*Rh complex, [1-butenyl-2-phenyl-1-(p-phenol)-1'-p-phenyl-(oxotrimethylene-3-dimethylamino)($\eta^1$-N-$\eta^5$-pentamethylcyclopentadienyl-rhodium)($\eta^1$-O-(CH_3OH)(OTf)](OTf), **cis**-**4(CH_3OH)** and **trans**-**5(CH_3OH)**, which were elucidated from their ^{1}H NMR spectra, and particularly, from the dramatic downfield shifts of the -N($CH_3$)_2 groups; 2.24/2.28 ppm **(1/2)** to 2.88($\Delta\delta$ = 0.64 ppm)/2.95($\Delta\delta$ = 0.67 ppm) ppm, **cis**-**4(CH_3OH)** and **trans**-**5(CH_3OH)**, respectively, while the $CH_2$N(CH_3)_2 was also shifted downfield $\sim$0.70 ppm; density functional theory (DFT) calculations showed that the monocation, with one OTf$^-$ binding to Cp*Rh, was more stable.[6]

Moreover, the N($CH_3$)_2 groups were doublets with $J_{H-Rh}$ = 5.0 Hz for both the **cis**-**4(CH_3OH)** and **trans**-**5(CH_3OH)** isomers, while the (-$CH_2$)N group was also a multiplet, because of coupling with Rh. The NMR data clearly showed the nitrogen atom as the kinetic binding site for Cp*Rh. More pertinently, the ^{1}H NMR (CD_3OD-d_4) spectrum of complex **cis**-**4(CH_3OH)** also showed that the resonance for the methylene group $\alpha$ to the oxygen, on the phenyl ether tether, -Ph-O-$CH_2$, was found to be shifted 0.11 ppm downfield in comparison to the free *cis*-hydroxytamoxifen ligand, **1**; presumably, a weak interaction of the ether oxygen and the Cp*Rh center, since no $J_{H-Rh}$ couplings were observed. This amplifies our present and original data that confirmed the principal finding that the dimethylamino group bound to the Cp*Rh center, where the $(CH_3)_2$N was shifted 0.64 ppm downfield, was the primary initial bonding mode. These experimental facts also seemed to further corroborate the recently reported DFT calculations of one of three plausible $\eta^2$-N,O

(3) (a) Fish, R. H. *Coord. Chem. Rev.* **1999**, *185/186*, 569, and references therein. (b) Fish, R. H. In *Bioorganometallics*; Jaouen, G., Ed.; Wiley-VCH: Weinheim, Germany, 2005; Chapter 10, p 321.
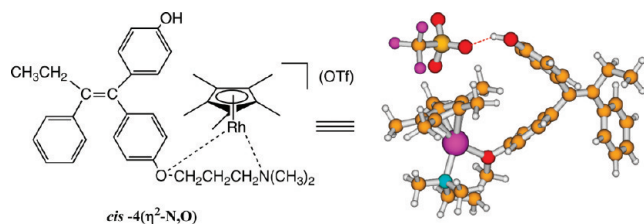
(4) Top, S.; Vessières, A.; Jaouen, G.; Fish, R. H. *Organometallics* **2006**, *25*, 3293.

(5) Vessières, A.; Top, S.; Pigeon, P.; Hillard, E.; Boubeker, L.; Spera, D.; Jaouen, G. *J. Med. Chem.* **2005**, *48*, 3937, and references therein.

(6) (a) Efremenko, I. E.; Top, S.; Martin, J. L. M.; Fish, R. H. *Dalton Trans.* **2009**, 4334.
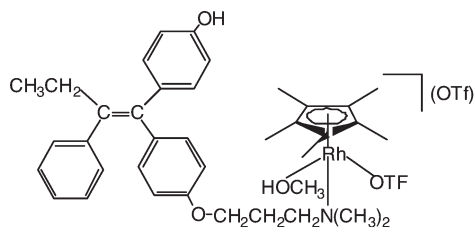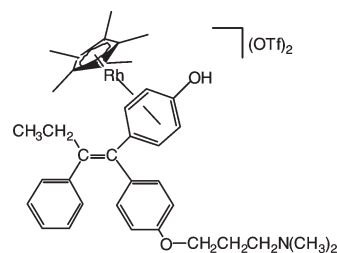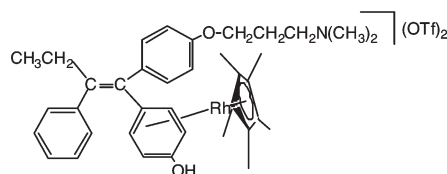
***cis*-4(CH₃OH)**
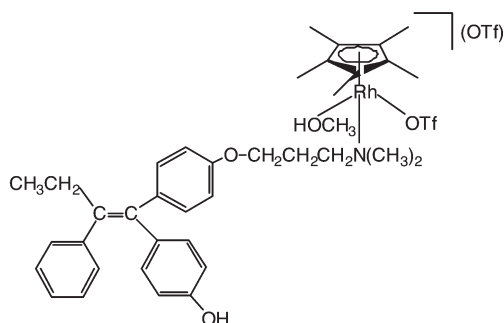
***trans*-5(CH₃OH)**

intermediates, ***cis*-4($\eta^2$-N,O)**, being formed at RT in CH₂Cl₂.[6]

***cis*-4($\eta^2$-N,O)**

More importantly, and in a serendipitous manner, we found upon individually heating complex ***cis*-4(CH₃OH)** or ***trans*-5(CH₃OH)** in CD₃OD-d₄ at 60 °C, a novel, and unprecedented N-$\pi$ rearrangement occurred that gave, after in-depth HMQC, HMBC, COSY, and NOESY correlation NMR studies, the *cis* or *trans*-[1-butenyl-2-phenyl-1-($\eta^5$-pentamethylcyclopentadienyl-$\eta^6$-*p*-phenol)rhodium)-1′-*p*-phenyl-(oxotrimethylene-3-dimethylamino)](OTf)₂, respectively, complex ***cis*-6** or ***trans*-7**. Thus, for example, the selective ¹H NMR upfield shifts for the signals at 5.25 ppm (H19, H21), and 6.32 ppm (H18, H22) for ***trans*-7**, clearly defined complexation of the Cp*Rh group exclusively to the phenol aromatic ring. Furthermore, for ***trans*-7**, the ¹³C NMR spectrum showed carbons 17, 18, 22, 19, and 21 as doublets with $J_{C-Rh}$ = 5.1 and 5.9 Hz, respectively. The quaternary carbon of the Cp* ring showed $J_{C-Rh}$ = 7.3 Hz (the *J* value was found to be dependent on the distance between the atoms involved). For ***cis*-6**, the following $J_{C-Rh}$ = 4.9 Hz for C11, 6.0 Hz for C12, 16, 13, 15, and 7.5 Hz for the Cp* ring were evident. These $J_{C-Rh}$ values further proved, unequivocally, that the Cp*Rh was $\eta^6$ bound to the phenol ring. The NOESY correlation NMR experiment is shown in Figure 1 (partial spectrum; see eq 1 for the numbering system), where ***trans*-7** demonstrated an NOE interaction

between the methylene protons and the methyl protons of the ethyl group, H3 and H4, 2.34 ppm and 0.71 ppm, respectively, with the aromatic proton resonance at 7.49 ppm, which were the protons, H12 and H16, of the uncomplexed phenyl ether ring (see the Supporting Information for all NMR Correlation Spectra).

In addition, we found that at 60 °C in CD₃OD-d₄, the $\eta^1$-N complexes, ***cis*-4(CH₃OH)** or ***trans*-5(CH₃OH)**, isomerized to a *cis* and *trans* mixture, during the N-$\pi$ rearrangement, but since both simultaneously undergo the N-$\pi$ rearrangement, it was difficult to obtain an accurate ratio for ***cis*-4(CH₃OH)**/***trans*-5(CH₃OH)**, after reaction. For example, after heating ***cis*-4(CH₃OH)** for 40 h at 60 °C, the ratio ***cis*-4(CH₃OH)**/***trans*-5(CH₃OH)** was found to be 10:1, while a similar experiment starting with complex ***trans*-5(CH₃OH)**, gave a ***cis*-4(CH₃OH)**/***trans*-5(CH₃OH)** ratio of 1:1; this thermodynamic fact was corroborated by DFT calculations that defined the ***cis*-4(CH₃OH)** more stable in CH₃OH than ***trans*-5(CH₃OH)**.[6]

***cis*-6**

***trans*-7**

It also appeared qualitatively from our ¹H NMR studies that this N-$\pi$ rearrangement was more favorable with ***trans*-5(CH₃OH)**, (with the aromatic ether tether *cis* to the ethyl on the double bond), rather than the corresponding, ***cis*-4(CH₃OH)**, on thermodynamic grounds.[6] We found that starting with ***cis*-4(CH₃OH)**, we observed the two $\eta^6$-Cp*Rh complexes, ***cis*-6** and ***trans*-7**, via NMR analysis of the new dimethylamino signals that appeared at 2.97 and 2.95 ppm, respectively, in the ratio of ~5:1, after 17 h of heating at 50 °C in CD₃OD-d₄, reflecting the isomerization of ***cis*-4(CH₃OH)** to ***trans*-5(CH₃OH)** prior to the N-$\pi$ rearrangement, as stated above. This propensity for the hydroxytamoxifen compounds, and its derivatives, to isomerize in organic solvents, has been previously studied by ¹H NMR; for example, *cis*-ferrocifen, **3**, in DMSO-d₆ and benzene-d₆, showed no *trans* isomer after one day at RT, while in CDCl₃ and acetone-d₆, there was a 1:1 and 3:7 *cis*/*trans* ratio, respectively.[2a]

Moreover, there was a dramatic solvent effect on the rate of the N-$\pi$ rearrangement.[4] We discovered that in CH₂Cl₂ the N-$\pi$ rearrangement, starting with the in situ formed $\eta^1$-N complex, **4(OTf)**, was completed in 15 h at
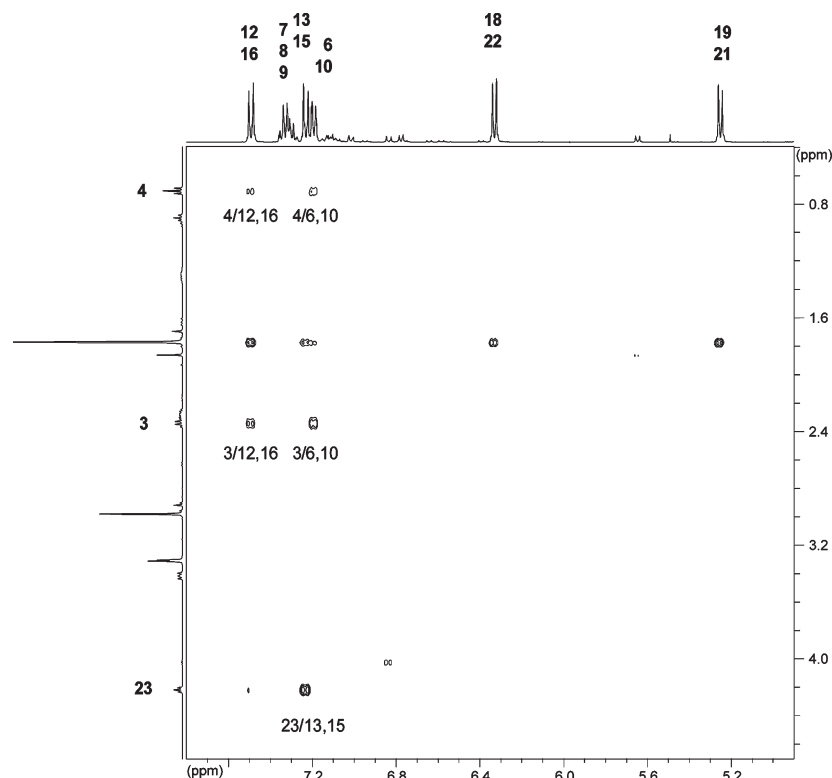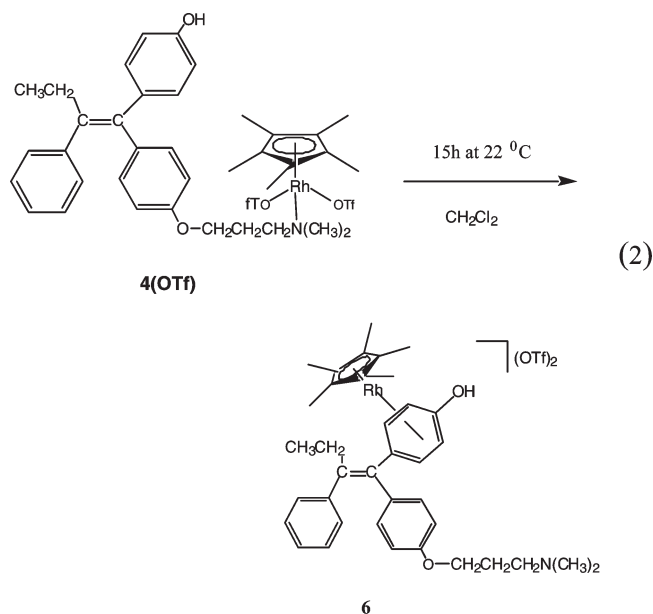
**Figure 1.** Partial Spectrum of the NOESY ^{1}H NMR Correlation Experiment of ***trans*-7** in CD$_3$OD-d$_4$.

22 °C for both ***cis*-4(OTf)** and ***trans*-5(OTf)** to either ***cis*-6** or ***trans*-7** (eq 2), while in CH$_3$OH *no reaction* occurred at 22 °C; *under these mild reaction conditions in CH$_2$Cl$_2$, neither **cis-4(OTf)** nor **trans-5(OTf)** was isomerized to a cis and trans mixture of both starting complexes.*



(2)

Importantly, we have also shown, in a recently published paper, utilizing DFT calculations, that this facile N-$\pi$ rearrangement in CH$_2$Cl$_2$ was conceivably due to the unusual role of the weaker binding triflate anion (OTf$^-$) complex of ***cis*-4(OTf)**; that is, OTf$^-$ was a better leaving group for the N-$\pi$ rearrangement in comparison to the thermodynamic

stability of ***cis*-4-(CH$_3$OH)** and ***trans*-5-(CH$_3$OH)** at RT.[6] Interestingly, complex ***cis*-6** was less stable to isomerization than ***trans*-7**. Thus, in CH$_2$Cl$_2$, complex ***cis*-6** gave a 9:1 ratio of ***cis*-6**:***trans*-7**, after being heated for 1 h at 40 °C, and then kept at 22 °C for 15 h, while complex ***trans*-7** did not show this isomerization propensity, under the same reaction conditions, and was verified by DFT calculations.[6]

It was also found that the $\eta^6$-Cp*Rh complexes, ***cis*-6** and ***trans*-7**, were *water-soluble*, via extraction of the reaction mixture, after removing CD$_3$OD-d$_4$, with D$_2$O, while the $\eta^1$-N-Cp*Rh bound, kinetic compounds, ***cis*-4(CH$_3$OH)** and ***trans*-5(CH$_3$OH)**, were *water insoluble; DFT calculations verified that these $\eta^1$-N complexes were monocations, and more hydrophobic, in comparison to the more hydrophilic, dicationic $\eta^6$ complexes.*[6] This also represented a rather facile technique for the separation of the $\eta^1$-N-Cp*Rh bound, kinetic products from the thermodynamic $\eta^6$ complexes, and moreover, provided the first water-soluble organometallic complexes of hydroxytamoxifen derivatives, ***cis*-1** and ***trans*-2**, to be synthesized, as far as we were able to ascertain, and boded well for possible increased biological compatibility. We also studied the isomerization of ***cis*-6** to ***trans*-7** as a function of pD (pH + 0.4) in D$_2$O (initial pD = 9.2) at RT, via ^{1}H NMR spectroscopy (Figure 2). The ***trans*-7** complex was preferred, as we raised the pD (NaOD) of a 46/54, ***cis*-6** (Cp*, 1.82 ppm)/***trans*-7**(Cp*, 1.71 ppm) mixture (initially dissolving pure ***cis*-6**) from 9.2 to 10.4 (20/80, ***cis*-6**/***trans*-7**). Therefore, the p$K_a$ of the phenol hydrogen was apparently lowered by the complexation to the $\eta^6$-Cp*Rh group, and facilitates the *cis* to *trans* isomerization at a lower pH versus free phenol (p$K_a$ = 10).
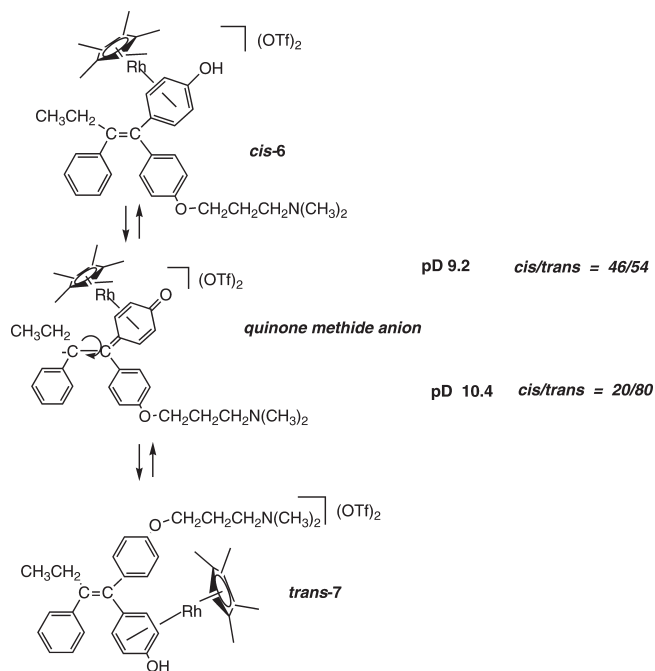
The N-π rearrangement was somewhat reminiscent of previous studies by Fish et al.[7] and Grotjahn et al.[8] with CpRu and Cp*Ru substituted pyridine/quinoline/benzothiophene/aliphatic amino and thio aromatic compounds that undergo a N-π or S-π rearrangement. However, the N-π rearrangement we have observed with *cis*-**4(OTf, CH₃OH)** and *trans*-**5(OTf, CH₃OH)** was unprecedented, as far as the past and current literature was concerned, since the Cp*Rh group has a choice between two geminal, electron-rich, oxygen substituted phenyl groups on the double bond; that is, the phenyl group with the ether, dimethylamino tether containing the $\eta^1$-N-Cp*Rh moiety, or the geminal phenol. Interestingly, we *exclusively* saw the regioselective $\eta^6$-Cp*Rh phenol complexes, *cis*-**6** or *trans*-**7**, being formed from *cis*-**4(OTf, CH₃OH)** and *trans*-**5(OTf, CH₃OH)**, respectively. The recent DFT study clearly showed that the phenol ring was more electron-donating, and that *cis*-**6** and *trans*-**7** were the thermodynamically most stable complexes that formed.[6]

To prove the *intramolecular* nature of the N-π rearrangement, we conducted a crossover experiment with complex *trans*-**5(OTf)** in the presence of compound **8**, and in CH₂Cl₂ at RT, for 20 h. If the N-π rearrangement, *trans*-**5(OTf)** to *trans*-**7**, was *intramolecular*, we should ideally see no Cp*Rh complexes of compound **8**; a control experiment with **8** and [Cp*Rh(H₂O)₃](OTf)₂, in CH₂Cl₂, showed an instantaneous reaction, with only one product formed, that being the regioselective $\eta^6$-Cp*Rh phenol complex, *trans* to the ethyl group, **9**, which was confirmed by correlation NMR studies.



**9**
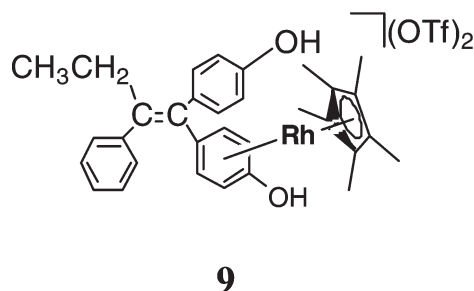
As stated, the crossover experiment was conducted with *trans*-**5(OTf)** in the presence of compound **8**, and in CH₂Cl₂ at RT, for 20 h. The ¹H NMR spectrum of the reaction mixture mainly showed the starting *trans*-**5(OTf)**, ~50%, while *trans*-**7**, *cis*-**6**, *cis*-**4(OTf)**, and a small amount of **9** were all present in ~50% yield. Thus, *trans*-**7** was the most important compound formed, as was stated above. Surprisingly, we also observed the isomerization of *trans*-**5(OTf)** giving a ratio of *trans*-**5(OTf)**/*cis*-**4(OTf)** = 7:1. In comparison to eq 2, where we saw no isomerization of *cis*-**4(OTf)** to *trans*-**5(OTf)**, in the formation of *cis*-**6**, we surmised that the acidic nature of **8** was possibly responsible for this isomerization. The formation of *cis*-**4(OTf)**, also led to the formation of *cis*-**6** (ratio of *trans*-**7**/*cis*-**6** = 3:1). Complex **9** was also present, while the ratio between *trans*-**7** and *cis*-**6**, to **9** was 3:1.

More importantly, if the N-π rearrangement, *trans*-**5(OTf)** to *trans*-**7**, was *intermolecular*, we should see

(7) Fish, R. H.; Kim, H.-S.; Fong, R. H. *Organometallics* **1991**, *10*, 770. (b) Fish, R. H.; Fong, R. H.; Tran, A.; Baralt, E. *Organometallics* **1991**, *10*, 1209.
(8) (a) Grotjahn, D. B. *Coord. Chem. Rev.* **1999**, *190−192*, 1125. (b) Grotjahn, D. B.; Joubran, C.; Combs, D.; Brune, D. C. *J. Am. Chem. Soc.* **1998**, *120*, 11814.



**Figure 2.** Isomerization of complex *cis*-**6** to *trans*-**7**, as a function of pD (pH + 0.4).

compound **9** in greater proportions compared to *trans*-**7** and *cis*-**6**, as the formation of this compound was very fast compared to the formation of *trans*-**7** or *cis*-**4(OTF)**. This was not the case, and consequently, *the intramolecular N-π rearrangement, must be the favored process* (eq 3).
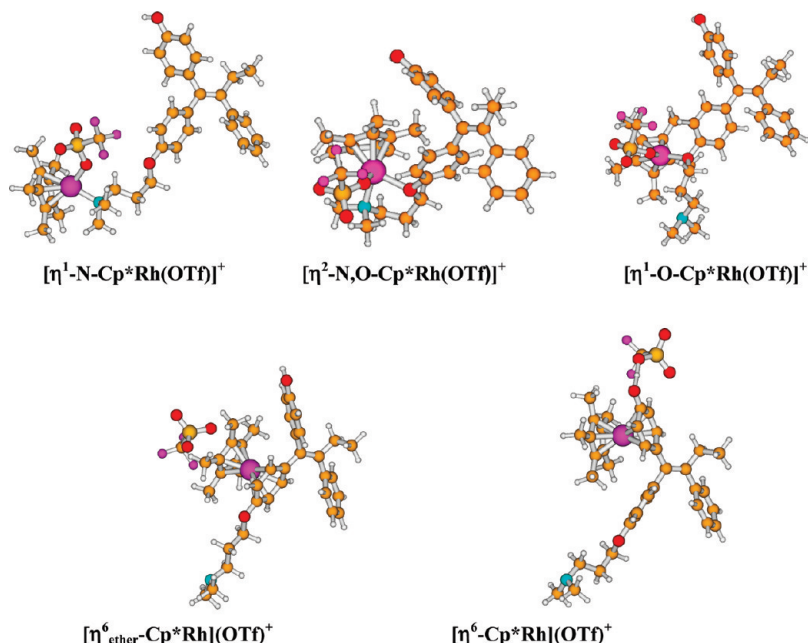


(3)
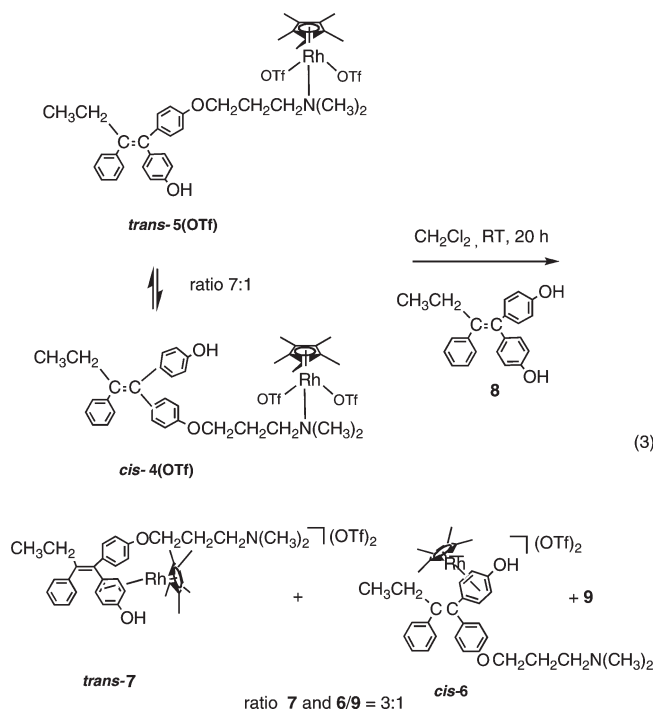
This latter result also provided added validity from recently reported DFT calculations, which defined the intramolecular pathway to ultimately form the $\eta^6$-Cp*Rh complexes, *trans*-**7** or *cis*-**6**.[6] The intermediates for the intramolecular and regioselective N-π rearrangement included

**Figure 3.** Optimized ground state conformations related to the N-$\pi$ conversion of *cis*-**4(OTf)** to *cis*-**6**. C(orange); H(white); N(blue); O(red); Rh(purple).

**Scheme 1.** Plausible Reaction Mechanism for the N-$\pi$ Rearrangement[a]
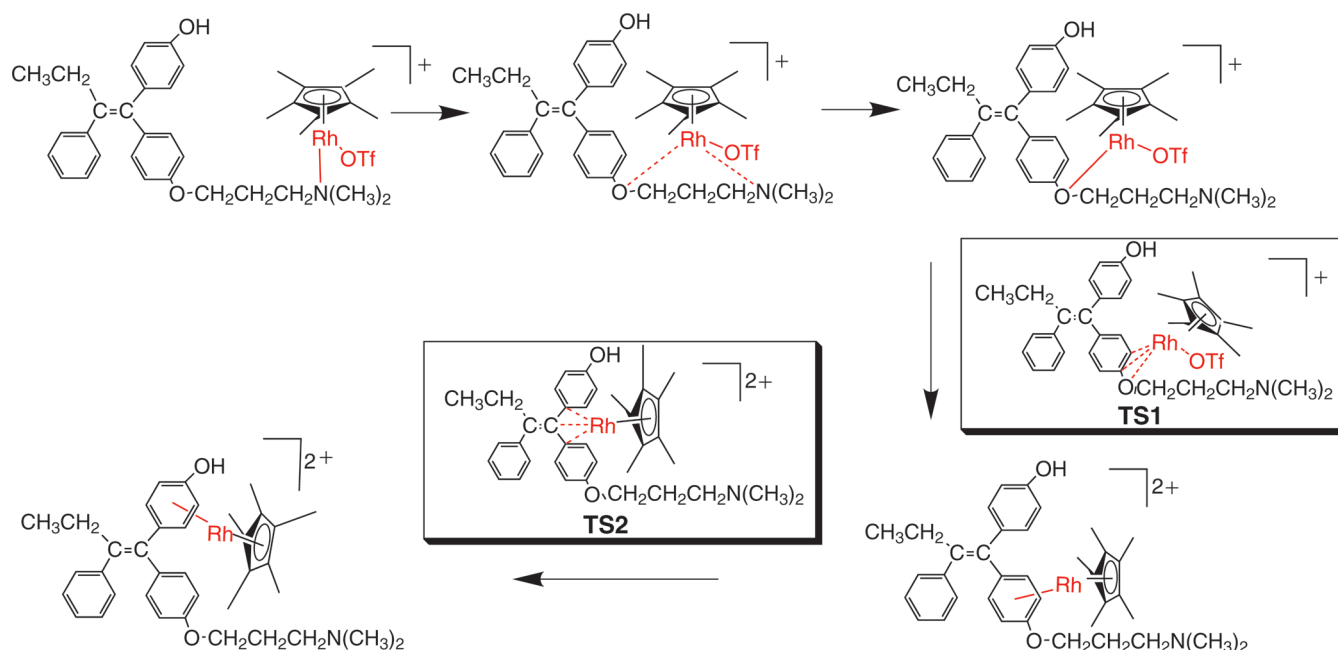


[a] Outer sphere counterions are omitted for clarity. TS1 and TS2 are the calculated transition states.[6]

the following complexes: $\eta^1$-N; $\eta^2$-N,O; $\eta^1$-O; an $\eta^6$ complex on the ether tether, and the final $\eta^6$-Cp*Rh-hydroxytamoxifen complex, which are shown in their optimized geometries (Figure 3).[6]

**Mechanism of the N-$\pi$ Rearrangement.** The intramolecular and regioselective N-$\pi$ rearrangement involved both the monocationic Cp*Rh—N complex and the inner sphere Cp*Rh-OTf bond dissociations as highly important steps. The geometries of the complexes that existed in $CH_2Cl_2$ and $CH_3OH$ solutions, including their recently derived DFT calculated energies, allowed us to determine

the lowest energy pathway for this novel transformation.[6] This pathway has been summarized as follows: Thus, the most plausible mechanism for the N-$\pi$ rearrangement is shown in Scheme 1. In both solvents, the rearrangement started from the monocationic, [$\eta^1$-N-Cp*Rh(OTf)]$^+$ (see conformational structures in Figure 3). The next step of the reaction consisted of the weakening of the Cp*Rh—$N_{amino}$ bond by formation of an additional Cp*Rh—$O_{ether}$ bond. The resulting complex, [$\eta^2$-N,O-Cp*Rh(OTf)]$^+$ (Figure 3), provided the resting state for this system, while its formation was very rapid in both solvents at high temperature;

at RT it was endothermic by 2–3 kcal/mol. The structurally flexible hydroxytamoxifen ligand, with a three methylene spacer, further provided that such interactions were sterically favored.

Upon cleavage of the activated Cp*Rh–N bond in complex $[\eta^2\text{-}\mathbf{N,O\text{-}Cp*Rh}](\mathbf{OTf})]^+$ (see ***cis*-4**($\eta^2$-**N,O**)), this then resulted in the formation of the monocationic complex, $[\eta^1\text{-}\mathbf{O\text{-}Cp*Rh})(\mathbf{OTf})]^+$. This complex was much less stable, from DFT calculations,[6] than the $\eta^1$-N and $\eta^2$-N,O complexes and, to complete the 18e- configuration, the Cp*Rh moiety moved toward the nearest neighboring aromatic ring. The rearrangement of the Cp*Rh group to the ether aromatic ring, $[\eta^6_{\text{ether}}\text{-}\mathbf{Cp*Rh}](\mathbf{OTf})^+$, proceeded with a significant gain in energy. However, in contrast to the previous stages, which represented the formation and dissociation of the metal–ligand bonds, that were typically barrierless, intramolecular migration of the Cp*Rh group afforded an activation pathway. In the transition state, **TS1** (Scheme 1), the Cp*Rh group formed two new bonds with the ether aromatic ring, while the Cp*Rh–O and Cp*Rh-OTf bonds were then

weakened. The calculated activation barriers for the $[\eta^1\text{-}\mathbf{O\text{-}Cp*Rh}(\mathbf{OTf})]^+ \rightarrow [\eta^6_{\text{ether}}\text{-}\mathbf{Cp*Rh}](\mathbf{OTf})^+$ transition were only 4.0 and 3.5 kcal/mol in $CH_2Cl_2$ and $CH_3OH$ solutions, respectively, at RT.[6] However, with respect to the lowest energy $\eta^1$-N complex, these values translated into 19.9 and 20.4 kcal/mol, respectively. Such an apparent activation barrier was consistent with the experimentally observed rate of the N-$\pi$ rearrangement.

Another possible scenario for the transformation of the $\eta^2$-N,O complex, $[\eta^2\text{-}\mathbf{N,O\text{-}Cp*Rh}(\mathbf{OTf})]^+$, was the endothermic loss of the inner sphere OTf⁻ ligand, leading to the outer sphere complex, $[\eta^2\text{-}\mathbf{N,O\text{-}Cp*Rh}](\mathbf{OTf})^+$, in which a coordinatively unsaturated, 16e- Cp*Rh center was still bound to both the $N_{\text{amino}}$ and $O_{\text{ether}}$ atoms. The energy cost of this reaction was found to be 10.08 and 9.85 kcal/mol in $CH_2Cl_2$ and $CH_3OH$ solutions, respectively. However, further transitions along this reaction pathway were energetically unfavorable with the $\eta^1$-O complex being 40.87 and 33.75 kcal/mol higher in energy than the lowest energy $\eta^1$-N complex in $CH_2Cl_2$ and $CH_3OH$ solutions, and with prohibitively high activation barriers, 42.18 and 35.07 kcal/mol, respectively.[6] Therefore, the Cp*Rh-OTf bond cleavage reaction directly precedes the formation of the $\eta^6$ complexes (**TS1**, Scheme 1).

Furthermore, during the last important step of the N-$\pi$ rearrangement, the Cp*Rh group was thermodynamically driven from the ether aromatic ring toward the geminal phenol ring, leading to the formation of the final monocationic *cis* complex, $[\eta^6\text{-}\mathbf{Cp*Rh}](\mathbf{OTf})^+$, which represented the most stable $\eta^6$ species in both solvents. In the transition state, **TS2** (Scheme 1), the Cp*Rh group was $\eta^1$-bonded to both aromatic rings, and to the carbon atom of the ethylene group. The calculated activation barrier, from the DFT studies, for this transition, was

**Table 1.** Relative Binding Affinities Values (RBA) of ***cis*-6** and ***trans*-7** at the Two Isoforms of the Estrogen Receptor, ER$\alpha$ and ER$\beta$, and Growth Inhibition Effects of ***cis*-6** on the Hormone Dependent (MCF-7) and Hormone Independent (MDA-MB-231) Breast Cancer Cell Lines

| | RBA (%)[a] | | $IC_{50}$ ($\mu$M)[b] | |
|---|---|---|---|---|
| complex | ER$\alpha$ | ER$\beta$ | MCF-7 ER$\alpha$ (+) malignant | MDA-MB-231 ER$\alpha$ (-) malignant |
| ***cis*-6** | $4.6 \pm 0.9$ | $2.6 \pm 0.3$ | 1.25 | 11 |
| ***trans*-7** | $0.8 \pm 0.2$ | $0.65 \pm 0.1$ | ND[c] | ND[c] |

[a] The mean of two experiments $\pm$ range. [b] after 5 days of culture. [c] Not Determined.
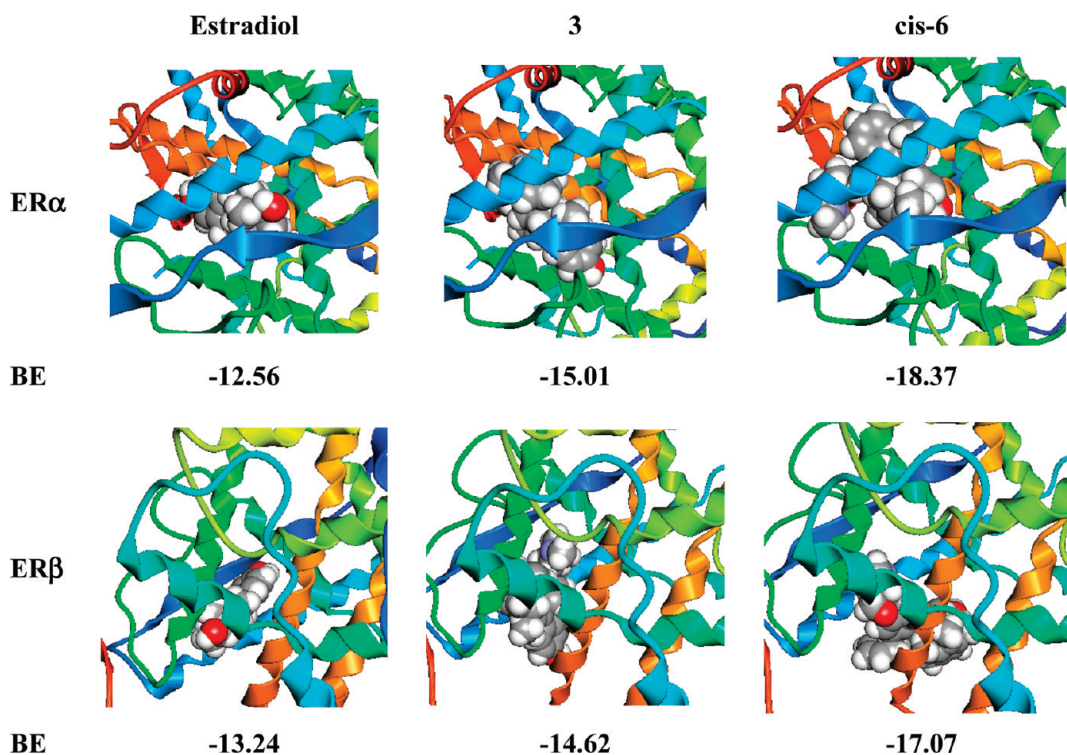


**Figure 4.** Cartoon representations of the ER$\alpha$ (top row) and ER$\beta$ (bottom row) receptor binding sites docked with estradiol, ferrocifen, **3**, and ***cis*-6**, together with the corresponding calculated binding energies (kcal/mol). The docked guests are shown in the CPK rendering mode.

**Table 2.** Guest-Estrogen Receptor Interaction Thermodynamics ($\Delta G$, kcal/mol) and H-Bond Lengths ($d_H$, Å) for Various Models of the ER$\alpha$ and ER$\beta$ Binding Sites Docked with Estradiol, Ferrocifen, **3**, and *cis*-**6**
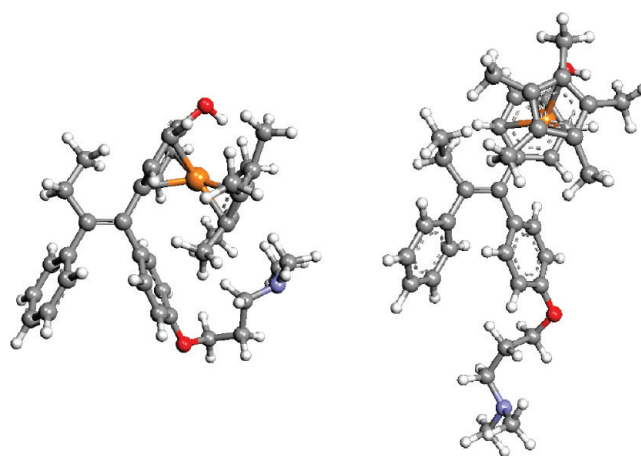
| | | estradiol | | | ferrocifen, **3** | | | *cis*-**6** | | | |
|---|---|---|---|---|---|---|---|---|---|---|---|
| ER$\alpha$ (**3ERD**)[b] | $\Delta G$ | **-12.56** | | | **-15.01** | | | **-18.37** | | | |
| | $d_H{}^a$ | 2.61 | 2.87 | 2.88 | 3.08 | 3.37 | | 3.00 | | | 2.81 |
| | atom | O | O | N | O | N | | O | | | O |
| | residue | Glu$_{353}$ | Gly$_{521}$ | His$_{524}$ | Leu428 | Val392 | | Leu$_{387}$ | | | Gly$_{521}$ |
| ER$\alpha$ (**1A52**) | $\Delta G$ | **-13.11** | | | **-14.74** | | | **-17.53** | | | |
| | $d_H$ | 2.78 | 3.00 | 3.00 | 2.86 | 3.31 | | No H-bonds | | | |
| | atom | O | O | N | O | O | | | | | |
| | residue | Arg$_{394}$ | Leu$_{391}$ | His$_{524}$ | Ser$_{395}$ | Leu$_{391}$ | | | | | |
| ER$\alpha$ (**1X7E**) | $\Delta G$ | **-13.20** | | | **-15.02** | | | **-19.29** | | | |
| | $d_H$ | 2.04 | 2.46 | | 1.84 | 2.26 | 3.02 | | 2.91 | | |
| | atom | O | O | | O | N | N | | N | | |
| | residue | Arg$_{394}$ | Phe$_{404}$ | | Met$_{421}$ | Phe$_{425}$ | Ile$_{424}$ | | Ala$_{350}$ | | |
| ER$\beta$ (**2FSZ**) | $\Delta G$ | **-13.24** | | | **-14.62** | | | **-17.07** | | | |
| | $d_H$ | 2.51 | 2.67 | 2.15 | No H-bonds | | | 2.84 | | 3.01 | |
| | atom | O | O | N | | | | O | | N | |
| | residue | Glu$_{305}$ | Glu$_{305}$ | Arg$_{346}$ | | | | Thr$_{299}$ | | Arg$_{346}$ | |
| ER$\beta$ (**1X78**) | $\Delta G$ | **-13.79** | | | **-14.63** | | | **-17.83** | | | |
| | $d_H$ | 2.54 | 2.97 | 2.98 | 2.03 | | | 3.12 | 3.12 | 2.29 | 2.93 |
| | atom | O | N | N | O | | | O | N | N | N |
| | residue | Glu$_{305}$ | His$_{475}$ | Arg$_{346}$ | Ala$_{302}$ | | | Met$_{336}$ | Met$_{340}$ | His$_{475}$ | Leu$_{476}$ |

$^a$ H-bond lengths indicate the distance between the nearest heavy atoms (not hydrogen), within 3.5 Å. $^b$ See the experimental section for X-ray structure designation, e.g., **3ERD** designates tamoxifen as the guest.
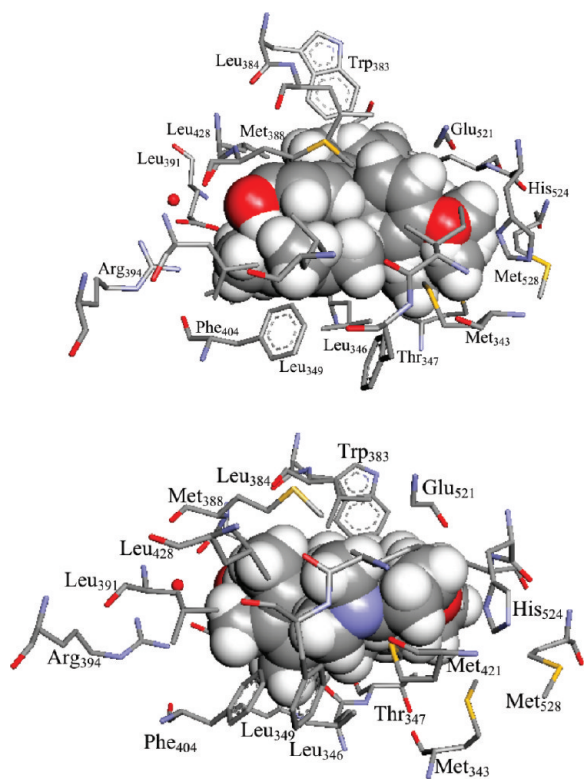
**Figure 5.** Amino acid residues within 5 Å of the ER$\alpha$ (top) and ER$\beta$ (bottom) receptor binding sites docked with *cis*-**6**.

**Figure 6.** Conformers adopted by the *cis*-**6** complex docked at the ER$\alpha$ (left) and ER$\beta$ (right) receptor binding sites.

16.33/16.22 kcal/mol in $CH_2Cl_2$/$CH_3OH$, at RT. Therefore, the Cp*Rh-OTf bond breaking step, in the transition state, **TS1** (Scheme 1), represented the rate-limiting step of the overall N-$\pi$ rearrangement process, in both solvents.[6]

These calculated DFT results suggested that [$\boldsymbol{\eta}^6$-**Cp*Rh**]-(**OTf**)$^+$ represented the most stable species in $CH_2Cl_2$ solution, at both room and higher temperatures. In contrast, in the more polar $CH_3OH$ solution, this complex represented the global minimum on the potential energy surface, only at elevated temperatures, while it was higher in energy than the initial complex, [$\boldsymbol{\eta}^1$-**N-Cp*Rh(OTf)**]$^+$, at RT. The entropy effect, and a fairly strong solvation of charged species in $CH_3OH$ solution, favored the dissociation of complex [$\boldsymbol{\eta}^6$-**Cp*Rh(OTf)**]$^+$, with formation of the dicationic [$\boldsymbol{\eta}^6$-**Cp*Rh**]$^{2+}$ complex as a main product in $CH_3OH$ solution. The solvato complex, [$\boldsymbol{\eta}^1$-**N-Cp*Rh(OTf)(CH$_3$OH)**]$^+$, was the most stable among those [$\boldsymbol{\eta}^1$-**N-Cp*Rh**] complexes that were considered in $CH_3OH$ solution, and it provided the most stable species in the system at RT. Thus, in spite of a different order of stability of the $\eta^1$-N and $\eta^6$ complexes, the DFT calculations indicated that the $\eta^1$-N complexes were more stable than the $\eta^6$ complexes in $CH_3OH$ solution at RT; therefore, no N-$\pi$ rearrangement would take place in $CH_3OH$ at RT, as was observed experimentally.

The proposed reaction pathway was very consistent with the experimental observations. The inner sphere coordination of the OTf$^-$ counterions in the initial $\eta^1$-N-Cp*Rh complexes agreed with their being insoluble in water. The Cp*Rh−N bond activation in these complexes
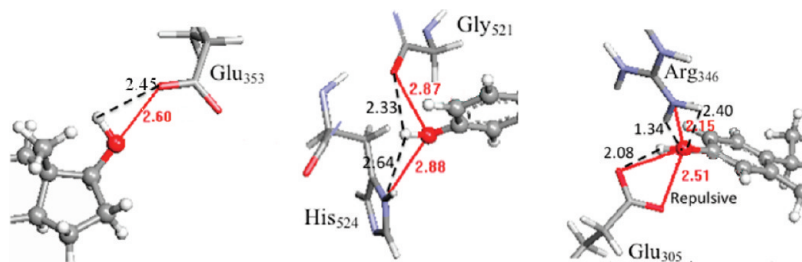
**Figure 7.** Detailed representations of non-covalent interactions between estradiol and ERα (**3ERD**, left and center), and ERβ (**2FSZ**, right).
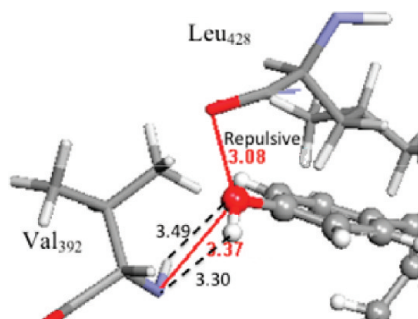


**Figure 8.** Detailed representation of non-covalent interactions between **3** and ERα.

by formation of the $\eta^2$-N,O complexes was confirmed by the small downfield shift of the -Ph-O-***CH_2***- protons, as observed via $^1$H NMR.

The higher solvation energy of the $\eta^6$ complexes in polar media was consistent with their water solubility, while the regioselectivity of the $\eta^6$ complexes that could form was in agreement with their relative stabilities.[6]

**Relative Binding Affinities of Complexes *cis*-6 and *trans*-7 for the ERα and ERβ Estrogen Receptors, and Growth Inhibition Properties of *cis*-6 with Breast Cancer Cell Lines.** Tamoxifen was found to be an antagonist breast cancer drug, that competitively inhibited the female hormone, estradiol, from binding to the hormone dependent ERα estrogen receptor, as one important aspect for anticancer activity.[2] Therefore, to determine the biological parameters of the water-soluble ***cis*-6** and ***trans*-7** complexes, the relative binding affinities (RBA) of these complexes for the two isoforms of the estrogen receptors (ERα and ERβ, 4 °C, 3 h) were determined by competition with [$^3$H]-estradiol, and provided values of 4.7% and 1%, respectively (Table 1).[4] Thus, it clearly showed a significant difference between the two geometrical isomers, ***cis*-6** and ***trans*-7**, which suggested differences in the binding conformation at the estrogen receptor. For comparison, ferrocifen, **3**, has an RBA of 11.5% (4 °C, 3 h).[2] Clearly, ***cis*-6** was found to be moderately competitive with estradiol for binding to the ERα receptor. Both compounds were recognized by the two isoforms of the estrogen receptor; however, the RBA values for the *cis* isomer, ***cis*-6**, on both isoforms of the receptor were significantly higher than those found for the *trans* isomer, ***trans*-7**.

The effect of the complex, ***cis*-6**, on the growth of cancer cells has been tested on two breast cancer cell lines, MCF-7 and MDA-MB-231, which are respectively, hormone dependent and hormone independent (Table 1). The ***cis*-6** complex showed a growth inhibition effect on these two cell lines with IC_{50} values in the range of 1.25−11 μM.

Thus, the ***cis*-6** isomer, which had a moderate RBA value, showed a antiestrogenic effect toward the MCF7 breast cancer cells, with a IC_{50} of 1.25 μM, and a antiproliferative effect toward the hormone independent MDA-MB-231 breast cancer cells, with an IC_{50} of 11 μM.

It was of interest to compare the IC_{50} values for the *cis* and *trans*-hydroxytamoxifen metabolites of tamoxifen, (with one less methylene group in the side chain than our ligands, ***cis*-1** and ***trans*-2**) with that of the ***cis*-6** complex for the antiestrogenic effect toward the MCF7 breast cancer cells, and the antiproliferative effect toward the MDA-MB-231 breast cancer cells. We found a wide range of reported IC_{50} values for a presumed 1:1 mixture of the *cis* and *trans* metabolites, 4-hydroxytamoxifen, but the classically obtained IC_{50} values for both cell line bioassays were in the range of ~18 μM against the MCF7 cancer cell line, and ~30 μM for the MDA-MB-231 cancer cell line.[9] Therefore, the ***cis*-6** complex, with one more methylene on the dimethylamino side chain, had a significantly lower IC_{50} value for growth inhibition of MCF7 cancer cells in comparison to the tamoxifen metabolites, *cis* and *trans*-4-hydroxytamoxifen, and similarly, a lower IC_{50} value for the growth inhibition of MDA-MB-231 cells. However, another important biological parameter of ***cis*-6** was its total water solubility, while the *cis* and *trans*-4-hydroxytamoxifen metabolites were found to be totally water insoluble. Presumably, lower doses of ***cis*-6** would be needed in any future in vivo experiments in comparison to the water insoluble *cis* and *trans*-4-hydroxytamoxifen metabolites, but more information is needed to ascertain the mode of action, and its in vivo activity, which will be the key to understanding its true potential as an anticancer drug.

**Computer Docking Studies of *cis*-6 at the Isoforms of the Estrogen Receptor, Hormone Dependent, ERα, and Hormone Independent, ERβ, Including Thermodynamic Values of Binding; Comparisons to Ferrocifen, 3, and the Female Hormone, Estradiol.** Since one important aspect of the bioactivity of all these potential organic, inorganic, and organometallic breast cancer drugs has been their action as an antagonist in competition with the female hormone, estradiol, we were interested in the binding modes of ***cis*-6**, the potent growth inhibitor we found against the MCF7 and MDA-MB-231 cell lines, at both the ERα and ERβ receptors, along with comparisons to two other guests, ferrocifen, **3**, and the female hormone itself, estradiol. Cartoon representations of the predicted three-dimensional (3D) structures of estradiol, ferrocifen, **3**, and ***cis*-6**, were

(9) See for example: Zhang, F.; Fan, P. W.; Liu, X.; Shen, L.; van Breemen, R. B.; Bolton, J. L. *Chem. Res. Toxicol.* **2000**, *13*, 53.
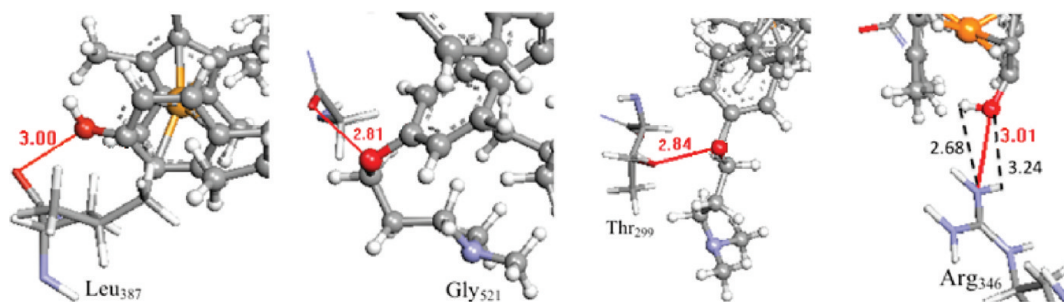
**Figure 9.** Detailed representations of the non-covalent interactions between *cis*-6 and ERα (**3ERD**, left two ) and ERβ (**2FSZ**, right two).

obtained using **3ERD** and **2FSZ** PDB structures as initial models of the ERα and ERβ receptor binding sites, respectively, and are shown in Figure 4, along with their corresponding binding energies. All the guests that are shown were bound in the pocket formed by helices H3, H4, H5, and H12, in a manner similar to that described before for other drugs.[10]

The docking results shown in Table 2 clearly demonstrated the negligible influence of the initial model used for the calculations of the binding energies of estradiol, ferrocifen, **3**, and *cis*-6, in both the ERα and the ERβ receptor binding sites. The guest compounds' orientations in both of the receptors' binding sites, determined by non-covalent bonding interactions, differed significantly for all the receptor models and their guests. Moreover, there was no dependence between the binding site box size and the interaction energy. While estradiol surprisingly showed a slightly higher affinity to the ERβ binding, a hormone independent receptor, ferrocifen, **3**, and *cis*-6, preferred the ERα binding site. Although different models provided somewhat different interaction energies, qualitatively, all the calculations indicated that guest-estrogen receptor interaction energies were in the following order: *cis*-6 > **3** > **estradiol**, for both the ERα and the ERβ receptor binding sites.

Detailed analysis of the *cis*-6 interactions with the ERα and ERβ receptor binding sites demonstrated that the main contribution to the host−guest interaction energy came from van der Waals and electrostatic interactions of the dicationic complex, *cis*-6, with the surrounding amino acids. Interaction of the phenol hydroxyl group, and the ether oxygen groups of *cis*-6 with O atoms of the surrounding amino acids, has generally been shown to have repulsive characteristics (Figure 5). More importantly, it also could possibly be the compact configuration adopted by the guest, *cis*-6, within the ERα host binding site, such that the electrophilic H atom of the phenol group was not readily available for non-covalent bonding regimes (Figure 6, left). In the less polar ERβ receptor binding site, the guest adopted a more open configuration (Figure 6, right).

A more detailed account of the non-covalent interactions that encompass estradiol, **3**, and *cis*-6, as designated in Table 2, for receptor binding to ERα and ERβ was as follows: Estradiol, the female hormone, was bound to its natural receptor site, and involved a significant contribution of non-covalent H-bonding interactions (Figure 7). In the case of the ERα binding site, the phenol oxygen, cyclopentanol oxygen, and their H atoms served as an

H-bond acceptor and donor (Glu$_{353}$, Glu$_{305}$, His$_{524}$). In the case of the ERβ binding site, only the phenol group was involved in the H-bonding interactions (Figure 7, Arg$_{346}$). Ferrocifen, **3**, bonding with ERα involved much weaker and longer H-bonds, in which the phenol OH group of the complex again served as both H-bond donor and acceptor in the non-covalent interactions with the amino group of Val$_{392}$ (Figure 8), while with the ERβ receptor, **3** did not show any non-covalent interactions within 3.5 Å.

The *cis*-6 non-covalent interactions with the ERα receptor binding site showed weak and long distance repulsive O−O interactions with Leu$_{384}$ and Gly$_{521}$ (Figure 9). In the case of the ERβ receptor binding site, the ether O atom showed a weak repulsion with Thr$_{299}$, while the phenol OH group was involved in a weak H-bond with Arg$_{346}$, and served as both H-bond donor and acceptor, although the H-bond donation seemed to be more pronounced.

**Conclusions**

We have reported on the synthesis of the Cp*Rh complexes of hydroxytamoxifen derivatives, *cis*-1 and *trans*-2, and in this process, we have discovered an unprecedented, intramolecular N-π rearrangement that was highly regiospecific for the geminal phenol group on the nucleus of complexes *cis*-4 and *trans*-5; recently published DFT calculations verified the optimized ground state conformations for the N-π rearrangement from complex *cis*-4 to *cis*-6, and helped define the intramolecular mechanism (Scheme 1), with bonding modes of $\eta^1$-N; $\eta^2$-N,O; $\eta^1$-O; and a $\eta^6$ complex on the ether tether (Figure 3).[6] Moreover, *cis*-6 showed a moderate competitive behavior toward estradiol at the ERα receptor versus *trans*-7. The water-soluble *cis*-6 complex was also found to be a growth inhibitor for hormone dependent MCF7 and hormone independent MDA-MB-231 breast cancer cells. Studies on the docking of *cis*-6 at the estrogen receptors, ERα and ERβ, also provided conformational information and thermodynamic data for these predominately van der Waals/electrostatic interactions, and demonstrated its stronger binding energy compared to the female hormone, estradiol, or ferrocifen, **3**.

Furthermore, we will continue these organometallic pharmaceutical studies, to further define the interactions of the complex, *cis*-6, and its Cp*Ru analogue, as potential probes for studying their binding interactions and the protein conformations at the estrogen receptor, ERα.[11] Another future

(10) Manas, E. S.; et al. *J. Am. Chem. Soc.* **2004**, *126*, 15106.

(11) (a) Sharmin, A.; Darlington, R. C.; Hardcastle, K. I.; Ravera, M.; Rosenberg, E.; Ross, J. B. A. *J. Organomet. Chem.* **2009**, *694*, 988. (b) Sharmin, A.; Rosenberg, E.; Ross, J. B. A.; Fish, R. H. unpublished results.

possible use of **cis-6** would be the synthesis of its Rh-105 radioisotope, a beta emitter, as a potential radiopharmaceutical. We feel that these representative bioorganometallic complexes, such as **cis-6** and **trans-7**, and their Cp*Ru analogues, could be used for these specific purposes, and hopefully will generate new directions for the bioorganometallic chemistry discipline.

## Experimental Section

All purchased starting materials and solvents were checked for purity. The NMR data were recorded at RT on a Bruker Avance 400 spectrometer operating at 400.1 and 100.6 MHz for $^1$H and $^{13}$C, respectively, and using a BBiz probe. The $^1$H and $^{13}$C chemicals shifts (TMS) were referenced to the residual solvent peaks. For all the compounds, assignments of individual resonances were achieved using a combination of one-dimensional (1D) and two-dimensional (2D) homo and hetero experiments; that is, COSY, HMQC, and HMBC. HMBC permits distinguishing the PhOH and PhOR aromatic groups for each compound, because of the long distance correlation between the protons, H-23 (the *Ph*O(CH$_2$)$_3$NMe$_2$ aromatic ring), and the quaternary aromatic carbons C-14 or C-20, for respectively, the **cis-6** or **trans-7** isomer, and similar HMBC and NOESY experiments that defined **cis-1**, **trans-2**, **cis-4**, **trans-5**, and **9**. This experiment also permitted assignments of all the other quaternary carbons. Finally, the NOESY experiment provided the unequivocal assignment of the **cis-6** or **trans-7** configurations for the $\eta^6$-Cp*Rh phenol ring binding site.

[Cp*Rh(solvent)$_3$](OTf)$_2$: $^1$H NMR Chemical Shifts (ppm) for Solvents, D$_2$O, CD$_3$OD, DMSO-d$_6$, and H$_2$O in CD$_2$Cl$_2$: $^1$H NMR (300 MHz): Cp*, 1.70 (CD$_2$Cl$_2$) ;1.58 (D$_2$O) ; 1.69 (CD$_3$OD); 1.53 (DMSO).

**Synthesis of *cis*-1 and *trans*-2**[5]. In a Schlenk tube, 1,1-dihydroxyphenyl-2-phenyl-but-1-ene (3.16 g, 10 mmol) was dissolved in anhydrous dimethylformamide (DMF, 30 mL). NaH (60% in oil, 1.51 g, 15 mmol) was then added as a powder into the solution, within 10 min. The solution was progressively heated to 100 °C (20 min). In another Schlenk tube, Et$_3$N (1.51 g, 15 mmol) was added to a suspension of Cl(CH$_2$)$_3$NMe$_2$.HCl (2.37 g, 15 mmol) in 30 mL of tetrahydrofuran (THF). After stirring for 1 h, the solution was filtrated and concentrated to 3 mL, and then 2 mL of DMF was added. This chloroamine solution was slowly added to the first solution maintained at 100 °C (10 min). After 1 h of heating, the mixture was allowed to cool to RT, and then 200 mL of ethyl acetate was added. The solution was washed with 2 × m_x00d7;50 mL of H$_2$O. After removal of the solvent, the crude product was first purified by silica gel flash column chromatography using acetone:Et$_3$N, 10:1 as eluent. Then 2.10 g mixture (1:1) of **cis-1** and **trans-2**, were isolated as an oil (52.5%), with 1.08 g of 1,1-dihydroxyphenyl-2-phenyl-but-1-ene being recovered (34%). *Cis*-1 and *trans*-2 were separated by semipreparative HPLC, using CH$_3$CN (with 1% Et$_3$N):H$_2$O, 80:20 as eluent. Isomers **cis-1** and **trans-2** were identified by COSY, NOESY, HMQC, and HMBC NMR correlation experiments. **Cis-1 Data:** $^1$H NMR (DMSO-d$_6$, 400 MHz): 0.84 (t, $J$ = 7.3 Hz, 3H, H-4), 1.74 (quint, $J$ = 6.7 Hz, 2H, H-24), 2.09 (s, 6H, N(CH$_3$)$_2$), 2.26 (t, $J$ = 7.1 Hz, 2H, H-25), 2.40 (q, $J$ = 7.3 Hz, 2H, H-3), 3.82 (t, $J$ = 6.4 Hz, 2H, H-23), 6.55 (d, $J$ = 8.7 Hz, 2H, H-19, H-21), 6.69 (d, $J$ = 8.7 Hz, 2H, H-18, H-22), 6.74 (d, $J$ = 8.4 Hz, 2H, H-13, H-15), 6.97 (d, $J$ = 8.4 Hz, 2H, H-12, H-16), 7.06−7.11 (m, 3H, H-8, H-6, H-10), 7.14−7.19 (m, 2H, H-7,H-9). $^{13}$C NMR (DMSO-d$_6$, 100 MHz) 13.6 (C-4), 27.1 (C-24), 28.7 (C-3), 45.4 (N(CH$_3$)$_2$), 55.8 (C-25), 65.6 (C-23), 113.4 (C-19, C-21), 115.1 (C-13, C-15), 126.1 (C-8), 128.1 (C-7, C-9), 129.6 (C-6, C-10), 130.3 (C-12, C-16), 131.6 (C-18, C-22), 134.1 (C-11), 135.5 (C-17), 138.1 (C-1), 140.1 (C-2), 142.4 (C-5), 156.3 (C-14) 156.7 (C-20). White crystals, mp 157 °C. Anal. Calc.

for C$_{27}$H$_{31}$NO$_2$,1/4 H$_2$O: C, 79.89 ; H, 7.81 ; N, 3.45. Found: C, 79.72 ; H, 7.73 ; N, 3.27.

***Trans*-2** Data: $^1$H NMR (DMSO-d$_6$, 400 MHz) 0.84 (t, $J$ = 7.4 Hz, 3H, H-4), 1.84 (quint, $J$ = 6.8 Hz, 2H, H-24), 2.14 (s, 6H, N(CH$_3$)$_2$), 2.35 (t, $J$ = 7.1 Hz, 2H, H-25), 2.39 (q, $J$ = 7.3 Hz, 2H, H-3), 3.99 (t, $J$ = 6.4 Hz, 2H, H-23), 6.39 (d, $J$ = 8.6 Hz, 2H, H-19, H-21), 6.59 (d, $J$ = 8.6 Hz, 2H, H-18, H-22), 6.90 (d, $J$ = 8.7 Hz, 2H, H-13, H-15), 7.06−7.11 (m, 5H, H-6, H-8, H-10, H-12, H-16), 7.15−7.19 (m, 2H, H-7, H-9). $^{13}$C NMR (DMSO-d$_6$, 100 MHz) 13.6 (C-4), 27.2 (C-24), 28.7 (C-3), 45.4 (N(CH$_3$)$_2$), 55.9 (C-25), 65.8 (C-23), 114.2 (C-13, C-15), 114.5 (C-19, C-21), 126.1 (C-8), 128.0 (C-7, C-9), 129.6 (C-6, C-10), 130.3 (C-12, C-16), 131.6 (C-18, C-22), 133.8 (C-17), 135.8 (C-11), 138.1 (C-1), 139.9 (C-2), 142.4 (C-5), 155.4 (C-20) 157.5 (C-14). White crystals, mp 183 °C. Anal. Calc. for C$_{27}$H$_{31}$NO$_2$,1/4 H$_2$O: C, 79.89 ; H, 7.81 ; N, 3.45. Found: C, 79.54; H, 7.81; N, 3.43.

**Reaction of *cis*-1, with in Situ Formed [Cp*Rh(CH$_3$OH)$_3$]-(OTf)$_2$ in CH$_3$OH: *cis*-4(CH$_3$OH).** In a Schlenk tube, 10 mg (0.025 mmol) of **cis-1** and 14 mg of [Cp*Rh(H$_2$O)$_3$](OTf)$_2$ (0.025 mmol) were dissolved in 2 mL of dry CH$_3$OH to form [Cp*Rh(CH$_3$OH)$_3$](OTf)$_2$, in situ, under Argon. The solution was stirred at RT for 15 min. A clear orange solution obtained was concentrated under vacuum to about 0.5 mL. Then, 10 mL of dry diethyl ether was added into the solution to precipitate **cis-4(CH$_3$OH)** as an orange oil. The mixture was left in a refrigerator for 1 h. The solution was stripped off, and the orange oil was washed with 2 mL of diethyl ether and dried under vacuum. Complex **cis-4(CH$_3$OH)** was isolated as an orange solid, 20 mg, 85% yield. $^1$H NMR (CD$_2$Cl$_2$, 400 MHz) 1.00 (t, $J$ = 7.4 Hz, 3H, H-4), 1.01 (s, 15H, (C$_5$(CH$_3$)$_5$), 2.15−2.20 (m, 2H, H-24), 2.55 (q, $J$ = 7.4 Hz, 2H, H-3), 2.90 (d, $J_{H-Rh}$ = 5.0 Hz, 6H, N(CH$_3$)$_2$), 3.24−3.45 (m, 2H, H-25), 3.98 (t, $J$ = 5.6 Hz, 2H, H-23), 6.60 (d, $J$ = 8.8 Hz, 2H, H-19, H-21), 6.83 (d, $J$ = 8.8 Hz, 2H, H-18, H-22), 7.10−7.22 (m, 5H, H-6, H-7,H-8, H-9, H-10), 7.26 (d, $J$ = 8.5 Hz, 2H, H-12, H-16), 7.44 (d, $J$ = 8.5 Hz, 2H, H-13, H-15). $^{13}$C NMR (CD$_2$Cl$_2$, 100 MHz) 7.4 (C$_5$(CH$_3$)$_5$), 13.2 (C-4), 24.3 (C-24), 29.1 (C-3), 43.4 (N(CH$_3$)$_2$), 56.0 (C-25), 64.0 (C-23), 90.2 (C$_5$(CH$_3$)$_5$), 113.0 (C-19, C-21), 121.8 (C-13, C-15), 127.6 (C-8), 127.7 (C-7, C-9), 129.5 (C-6, C-10), 130.3 (C-12, C-16), 131.7 (C-18, C-22), 136.2 (C-17), 137.7 (C-1, C-11), 140.9 (C-2), 142.3 (C-5), 156.0 (C-20), 163.1 (C-14). ESI-MS (ES): $m/z$: 639 [M$^+$ − 2CF$_3$SO$_3$$^-$].

**Reaction of *trans*-2 with in Situ Formed [Cp*Rh(CH$_3$OH)$_3$]-(OTf)$_2$ in CH$_3$OH: *trans*-5(CH$_3$OH).** In a Schlenk tube, 10 mg (0.025 mmol) of **trans-2**, and 14 mg of [Cp*Rh(H$_2$O)$_3$](OTf)$_2$ (0.025 mmol) were dissolved in 2 mL of dry CH$_3$OH to form [Cp*Rh(CH$_3$OH)$_3$](OTf)$_2$, under Argon. The solution was stirred at RT for 15 min and then the clear orange solution obtained was concentrated under vacuum to about 0.5 mL. Then, 10 mL of dry diethyl ether was added into the solution, to precipitate the complex as an orange oil. The mixture was left in a refrigerator for 1 h. The solution was stripped off, and the orange oil was washed with 2 mL of diethyl ether, and then dried under vacuum. The *trans*-$\eta^1$-N-complex, **5(CH$_3$OH)**, was isolated as an orange solid, 22 mg, 91% yield. $^1$H NMR (CD$_2$Cl$_2$, 400 MHz) 0.70 (s, 15H, (C$_5$(CH$_3$)$_5$), 0.98 (t, $J$ = 7.3 Hz, 3H, H-4), 2.25−2.29 (m, 2H, H-24), 2.53 (q, $J$ = 7.3 Hz, 2H, H-3), 2.96 (d, $J_{H-Rh}$ = 5.0 Hz, 6H, N(CH$_3$)$_2$), 3.33−3.38 (m, 2H, H-25), 4.12 (t, $J$ = 5.5 Hz, 2H, H-23), 6.79 (d, $J$ = 8.6 Hz, 2H, H-18, H-22), 6.91 (d, $J$ = 8.8 Hz, 2H, H-13, H-15), 6.93 (d, $J$ = 8.6 Hz, 2H, H-19, H-21), 7.07−7.10 (m, 1H, H-8), 7.12−7.18 (m, 6H, H-6, H-7, H-9, H-10, H-12, H-16). $^{13}$C NMR (CD$_2$Cl$_2$, 100 MHz) 7.1 (C$_5$(CH$_3$)$_5$), 13.0 (C-4), 24.3 (C-24), 28.5 (C-3), 43.3 (N(CH$_3$)$_2$), 55.9 (C-25), 64.2 (C-23), 89.7 (C$_5$(CH$_3$)$_5$), 113.6 (C-13, C-15), 120.9 (C-19, C-21), 125.5 (C-8), 127.4 (C-7, C-9), 129.5 (C-6, C-10), 130.2 (C-12, C-16), 131.5 (C-18, C-22), 136.4 (C-11), 137.4 (C-17), 137.8 (C-1), 140.9 (C-2), 142.8 (C-5), 156.8 (C-14), 163.8 (C-20). ESI-MS: $m/z$: 639 [M$^+$ − 2CF$_3$SO$_3$$^-$].

**Reaction of *cis*-1, with [Cp*Rh(H$_2$O)$_3$](OTf)$_2$ in CH$_2$Cl$_2$: $\eta^6$-Complex, *cis*-6.** In a Schlenk tube, 40 mg (0.10 mmol) of **cis-1**

and 55 mg of $[Cp*Rh(H_2O)_3](OTf)_2$ (0.10 mmol) were dissolved in 10 mL of dry $CH_2Cl_2$ under argon. The solution was stirred at 40 °C for 1 h and at RT for 15 h. The solution was filtrated and concentrated without heating to 1 mL. Then 4 mL of dry pentane were added leading to the formation of an orange oil. After 1 h in a refrigerator, the solvent was removed by decantation followed by pumping under vacuum to give an orange solid (89 mg, 95% yield, mp 140 °C). The $^1H$ NMR spectrum shows the formation of two $\eta^6$ complexes in the ratio **6:7** = 9:1. $^1H$ NMR (CD$_3$OD, 400 MHz) of *cis*-**6**: 0.94 (t, $J$ = 7.5 Hz, 3H, H-4), 1.86 (s, 15H, (C$_5$(CH$_3$)$_5$), 2.13−2.20 (m, 2H, H-24), 2.63 (q, $J$ = 7.5 Hz, 2H, H-3), 2.92 (s, 6H, N(CH$_3$)$_2$), 3.29−3.33 (m, 2H, H-25), 4.02 (t, $J$ = 5.8 Hz, 2H, H-23), 5.65 (d, $J$ = 7.5 Hz, 2H, H-13, H-15), 6.77 (d, $J$ = 7.5 Hz, 2H, H-12, H-16), 6.84 (d, $J$ = 8.7 Hz, 2H, H-19, H-21), 7.00−7.03 (m, 2H, H-6, H-10), 7.08−7.13 (m, 5H, H-7, H-8, H-9, H-18, H-22). $^{13}C$ NMR (CD$_3$OD, 100 MHz) 9.7 (C$_5$(CH$_3$)$_5$), 12.9 (C-4), 25.7 (C-24), 30.2 (C-3), 43.7 (N(CH$_3$)$_2$), 56.8 (C-25), 66.0 (C-23), 93.0 (d, $J_{C-Rh}$ = 6.1 Hz, C-13, C-15), 104.5 (d, $J_{C-Rh}$ = 6.0 Hz, C-12, C-16), 108.3 (d, $J_{C-Rh}$ = 7.5 Hz, C$_5$(CH$_3$)$_5$), 114.0 (d, $J_{C-Rh}$ = 4.9 Hz, C-11), 115.5 (C-19, C-21), 127.8 (C-8), 128.8 (C-7, C-9), 129.9 (C-6, C-10), 130.6 (C-1), 132.9 (C-18, C-22), 134.5 (C-17), 142.3 (C-5), 154.2 (C-2), 159.2 (C-20), 160.9 (C-14). ESI-MS: $m/z$: 788[M$^+$-CF$_3$SO$_3$H], 638[M$^+$ − 2CF$_3$SO$_3$H]. Anal. Calcd for C$_{39}$H$_{46}$F$_6$NO$_8$S$_2$Rh: C, 49.95; H, 4.94. Found. C, 49.22; H, 5.12. A NOESY experiment showed a correlation between H12 and H16 with the CH$_2$ protons of the ethyl group. As expected the signal of the CH$_2$ group at 2.63 correlated with the signal at 6.77, which was the signal of H12 and H16. We also observed a correlation of these aromatic protons with the methyl group at 0.94 ppm. In combination with the COSY experiment, this allowed the identification of all protons, especially H13 and H15 of the phenol group. The upfield shift of the phenol protons proved that this ring was selectively complexed by the Cp*Rh group.

**Reaction of *trans*-2 with [Cp*Rh(H$_2$O)$_3$](OTf)$_2$: $\eta^6$-Complex, *trans*-7.** In a Schlenk tube, 40 mg (0.10 mmol) of *trans*-**2** and 55 mg of $[Cp*Rh(H_2O)_3](OTf)_2$ (0.10 mmol) were dissolved in 10 mL of dry $CH_2Cl_2$ under argon. The solution was stirred at 40 °C for 1 h and at RT for 15 h. The solution was then filtered and concentrated, without heating, to 3 mL. Then, 8 mL of dry pentane was added leading to the formation of an orange oil. After 1 h in a refrigerator, the solvent was removed by decantation, followed by pumping under vacuum, giving an orange solid (81 mg, 86% yield, mp 130 °C). The NMR spectrum showed only one $\eta^6$ complex, *trans*-**7**. $^1H$ NMR (CD$_3$OD, 400 MHz) 0.71 (t, $J$ = 7.4 Hz, 3H, H-4), 1.77 (s, 15H, (C$_5$(CH$_3$)$_5$), 2.26−2.31 (m, 2H, H-24), 2.34 (q, $J$ = 7.4 Hz, 2H, H-3), 2.98 (s, 6H, N(CH$_3$)$_2$), 3.39−3.44 (m, 2H, H-25), 4.22 (t, $J$ = 5.7 Hz, 2H, H-23), 5.25 (d, $J$ = 7.7 Hz, 2H, H-19, H-21), 6.32 (d, $J$ = 7.7 Hz, 2H, H-18, H-22), 7.18−7.20 (m, 2H, H-6, H-10), 7.23 (d, $J$ = 8.2 Hz, 2H, H-13, H-15), 7.29−7.34 (m, 3H, H-7, H-8, H-9), 7.49 (d, $J$ = 8.6 Hz, 2H, H-12, H-16). $^{13}C$ NMR (CD$_3$OD, 100 MHz) 9.7 (C$_5$(CH$_3$)$_5$), 12.4 (C-4), 25.8 (C-24), 30.7 (C-3), 43.7 (N(CH$_3$)$_2$), 56.8 (C-25), 66.3 (C-23), 91.8 (d, $J_{C-Rh}$ = 5.9 Hz, C-19, C-21), 103.2 (d, $J_{C-Rh}$ = 5.9 Hz, C-18, C-22), 107.9 (d, $J_{C-Rh}$ = 7.3 Hz, C$_5$(CH$_3$)$_5$), 115.5 (d, $J_{C-Rh}$ = 5.1 Hz, C-17), 116.4 (C-13, C-15), 129.0 (C-8), 129.9 (C-7, C-9), 130.9 (C-6, C-10), 131.0 (C-1), 132.1 (C-12, C-16), 132.4 (C-11), 141.0 (C-5), 155.8 (C-2), 160.1 (C-14), 160.7 (C-20). ESI-MS: $m/z$: 788 [M$^+$ − CF$_3$SO$_3$H], 638 [M$^+$ − 2CF$_3$SO$_3$H]. Anal. Calcd for C$_{39}$H$_{46}$F$_6$NO$_8$S$_2$Rh: C, 49.95; H, 4.94. Found. C, 49.34; H, 5.07. A NOESY experiment showed a correlation between H12 and H16 with CH$_2$ protons of the ethyl group (Figure 1). As expected the signal of the CH$_2$ group at 2.34 ppm correlates with the signal at 7.49 ppm, which was the signal of H12 and H16. We also observed a correlation of these aromatic protons with the methyl group at 0.71 ppm. By combining the COSY experiment with the NOESY spectrum, this allowed the identification of all protons, especially H13 and H15 of the phenol group. The selective upfield shifts of the phenol protons proved that this ring was selectively complexed by Cp*Rh.

**HPLC Separations of Complexes: *cis*-1, *cis*-4, *cis*-6, *trans*-2, *trans*-5, and *trans*-7.** Column: Kromasil C18, 10 $\mu$m; L = 250 mm ; D = 4.6 mm.

Eluent: MeCN/H$_2$O with 0.1 TFA: 70/30; flow = 0.6 mL/min ; $\lambda$ = 254 nm.

| | |
|---|---|
| *cis*-**1** | rt = 5.91 min |
| *cis*-**4** | rt = 5.83 min |
| *cis*-**6** | rt = 3.65 min |
| *trans*-**2** | rt = 5.85 min |
| *trans*-**5** | rt = 5.67 min |
| *trans*-**7** | rt = 3.67 min |

With eluent: MeCN 1%Et$_3$N/H$_2$O: 80/20; flow = 1 mL/min.

| | |
|---|---|
| *cis*-**1** | rt = 8.05 min |
| *trans*-**2** | rt = 10.35 mi |

**$^1$H NMR Isomerization Experiment of *cis*-6 to *trans*-7 in D$_2$O as a Function of pD.** In a 5 mm NMR tube was placed 10 mg of *cis*-**6**, in 300 $\mu$L of D$_2$O. The pD was measured via an NMR tube fitting electrode and was found to be 9.2. The $^1H$ NMR spectrum showed at the initial pD of 9.2 that substantial isomerization had already occurred providing a 46 (Cp*, 1.82 ppm)/ 54 (Cp*, 1.71 ppm) ratio of *cis*-**6**/*trans*-**7**. The pD was then changed with NaOD to 10.4, and the spectrum recorded showed that the ratio was now 20/80, *cis*-**6**/*trans*-**7**.

**Reaction of *cis*-1 with in Situ [Cp*Rh(CD$_3$OD)$_3$](OTf)$_2$.** In a Schlenk tube, 40.1 mg (0.1 mmol) of *cis*-**1** was dissolved in 3 mL of CD$_3$OD, and then 55.0 mg of the aqua complex, [Cp*Rh(H$_3$O)$_3$]-(OTf)$_2$, to form in situ, [Cp*Rh(CD$_3$OD)$_3$](OTf)$_2$ (0.1 mmol), was added into the solution, and kept at RT. A clear orange solution was then obtained, while the reaction was monitored by $^1H$ NMR, and after 15 min, the signal of the NMe$_2$ protons moved downfield from 2.23 ppm to 2.90 ppm proving that this group binds to Cp*Rh. The aromatic protons did not show any significant change. The spectrum started to change when the solution was heated at 60 °C. After 40 h at 60 °C, the reaction was not complete, with complex **4** still the main compound in the solution, ratio of **4:6**, 60:40. Isomerization also occurred with ratio of **6:7**, 55:45. Complex **5** was also present in small amounts. The CH$_3$OH was removed, and the product was stirred with 2 mL of D$_2$O for 3 h. The $^1H$ NMR of the D$_2$O solution that separated the water-soluble $\eta^6$-complexes in the ratio of **6:7**, 45:55 (24 mg).

**Reaction of *Trans*-2 with [Cp*Rh(CD$_3$OD)$_3$](OTf)$_2$.** In a Schlenk tube, 20.0 mg (0.05 mmol) of *trans*-**2** was dissolved in 2.5 mL of CD$_3$OD-d$_4$, and then 28.0 mg of [Cp*Rh(H$_2$O)$_3$]-(OTf)$_2$ (0.05 mmol) was added into the solution and kept at RT, generating, [Cp*Rh(CH$_3$OH)$_3$](OTf)$_2$, in situ.

A clear orange solution was obtained. The reaction was monitored by $^1H$ NMR., and after 10 min, the signal for the NMe$_2$ group moved from 2.28 to 2.95 ppm, proving that this group binds to Cp*Rh. The aromatic protons did not show any significant change except that the phenol protons became broad. After 20 h at 60 °C, at least four products were present in the solution. The methanol was evaporated and the solid obtained was stirred with 1.5 mL of D$_2$O for 30 min. The $^1H$ NMR of the D$_2$O solution showed the mixture of the two $\eta^6$ complexes in the ratio of **6:7**, 75:25 (21 mg). After 20 h at 60 °C, the main compound in the solution was *trans*-**7**, with a *trans*-**5**:*trans*-**7** ratio of, 20:80. Isomerization also occurred with a *cis*-**6**:*trans*-**7** ratio of, 20:80. Complex *cis*-**4** was also present. The CH$_3$OH was removed, and the product was stirred with 2 mL of D$_2$O for 3 h. The $^1H$ NMR of the D$_2$O solution showed the mixture of the two $\eta^6$-complexes, *cis*-**6**:*trans*-**7** in a ratio of 45:55 (24 mg). CH$_3$OH was evaporated, and the solid obtained was stirred with 1.5 mL of D$_2$O for 30 min. $^1H$ NMR of the D$_2$O solution showed the

mixture of the two $\eta^6$-complexes in the ratio of *cis*-6:*trans*-7, 25:75 (21 mg).

**Reaction of 1,1-Di(4-hydroxyphenyl)-2-phenyl-but-1-ene with [Cp*Rh(H$_2$O)$_3$](OTf)$_2$: Regioselective $\eta^6$ Complex, 9.** In a Schlenk tube, 32 mg (0.10 mmol) of 1,1-di(4-hydroxyphenyl)-2-phenyl-but-1-ene was dissolved in 10 mL of dry CH$_2$Cl$_2$ under argon, and then 55 mg (0.10 mmol) of [Cp*Rh(H$_2$O)$_3$](OTf)$_2$ was added as a solid. An orange oil was formed immediately, and the mixture was then stirred at RT for another 3 h. The solution was concentrated at RT to ∼2 mL. Then, 1 mL of dry methanol was added, while the complex was precipitated by addition of 5 mL of dry pentane. The solid was washed with 0.5 mL of CH$_2$Cl$_2$ and 3 mL of pentane. The desired complex was obtained as an orange solid (25 mg, 29% yield). The $^1$H NMR spectrum showed only one $\eta^6$ isomer, complex **9**. $^1$H NMR (CD$_3$OD, 400 MHz) 0.72 (t, $J = 7.4$ Hz, 3H, H-4), 1.79 (s, 15H, (C$_5$(CH$_3$)$_5$), 2.37 (q, $J = 7.4$ Hz, 2H, H-3), 5.42 (d, $J = 7.4$ Hz, 2H, H-19, H-21), 6.41 (d, $J = 7.4$ Hz, 2H, H-18, H-22), 7.03 (d, $J = 8.2$ Hz, 2H, H-13, H-15), 7.16−7.19 (m, 2H, H-6, H-10), 7.28−7.34 (m, 3H, H-7, H-8, H-9), 7.37 (d, $J = 8.2$ Hz, 2H, H-12, H-16). $^{13}$C NMR (CD$_3$OD, 100 MHz) 9.7 (C$_5$(CH$_3$)$_5$), 12.4 (C-4), 30.7 (C-3), 92.0 (d, $J_{C-Rh} = 6.1$ Hz, C-19, C-21), 103.6 (C-18, C-22), 109.0 (C$_5$(CH$_3$)$_5$), 114.0 (C-17), 117.0 (C-13, C-15), 129.0 (C-8), 129.8 (C-7, C-9), 130.9 (C-11), 131.0 (C-6, C-10), 131.1 (C-1), 132.0 (C-12, C-16), 140.9 (C-5), 155.5 (C-2), 159.2(C-14), 160.4 (C-20). The NOESY experiment showed correlations between the ethyl group (H$_4$ at 0.72 and H$_3$ at 2.37 ppm) and the downfield phenol (H$_{12,16}$ at 7.37 ppm), providing selective $\eta^6$ complexation of Cp*Rh on the phenol group, which was *trans* to the ethyl group. MS (ES) *m/z*: 554 [M$^+$ − 2 CF$_3$SO$_3$].

**Crossover Experiment of *trans*-5(OTf) to trans-7, in the Presence of 1,1-Di(4-hydroxyphenyl)-2-phenyl-but-1-ene.** In a Schlenk tube, ***trans*-5(OTf)** (28 mg, 0.03 mmol) and 1,1-di(4-hydroxyphenyl)-2-phenyl-but-1-ene (10 mg, 0.03 mmol) were dissolved in 3 mL of dry CH$_2$Cl$_2$. The solution was stirred at RT for 20 h. The solvent was removed. The solid obtained was dissolved in CD$_3$OD, and the $^1$H NMR spectrum showed starting material, ***trans*-5(OTf)** (50%), while ***trans*-7**, ***cis*-6**, ***cis*-4(OTf)**, and **9** were also present in 50% yield. The ratios between compounds are ***trans*-5(OTf)**/***cis*-4(OTf)** = 7:1; ***trans*-7**/***cis*-6** = 3:1; (***trans*-7** and ***cis*-6**)/**9** = 3:1.

## Biological Experiments

**In Vitro Bioassays for *cis*-6.** Human breast cancer cell lines, MCF7 (ER(+), malignant) and MDA-MB-231 (ER(-), malignant), were obtained from the American Type Culture Collection (ATCC) and maintained in recommended media without phenol red. For the determination of IC$_{50}$ values for the indicated compounds, a 20 mM stock of each compound was prepared in DMSO. The freshly prepared stock solutions were then diluted with appropriate media for each cell line to achieve final concentrations between 0.2 and 20 $\mu$M. Growing cultures of subconfluent cells were subdivided by trypsinization and replated at a density of $3\times(10)^3$ cells/well in standard 24 well multiwell cell culture plates (Corning Costar). The diluted compounds were added to the cells 24 h after seeding. Three replicates were performed for each concentration. The cells were maintained in the presence of the compounds or the DMSO diluent control for 5 days, after which the cells in individual wells were detached by trypsinization, and counted using a Coulter Counter (Beckman Coulter). IC$_{50}$ values were then calculated from the plots of cell numbers (5 days) versus compound concentrations.

**Determination of the Relative Binding Affinity (RBA) of the *cis*-6 and *trans*-7, for ER$\alpha$ and ER$\beta$.** RBA values were measured on ER$\alpha$ from lamb uterine cytosol and on ER$\beta$ purchased from Pan Vera (Madison, WI, U.S.A.). Sheep uterine cytosol prepared in buffer A (0.05 M Tris-HCL, 0.25 M sucrose, 0.1% $\beta$-mercaptoethanol, pH 7.4 at 25 °CC) as previously described

was used as a source of ER$\alpha$.[8] For ER$\beta$, 10 $\mu$L of the solution containing 3500 pmol/mL were added to 16 mL of buffer B (10% glycerol, 50 mM Bis-Tris-Propane pH 9, 400 mM KCl, 2 mM DTT, 1 mM EDTA, 0.1% BSA) in a silanized flask. Aliquots (200 $\mu$L) of ER$\alpha$ in glass tubes or ER$\beta$ in polypropylene tubes were incubated for 3 h at 0 °C with [6,7-$^3$H]- estradiol ($2 \times 10^{-9}$ M, specific activity 1.62 TBq/mmol, NEN Life Science, Boston, MA) in the presence of nine concentrations of the hormones to be tested. At the end of the incubation period, the free and bound fractions of the tracer were separated by protamine sulfate precipitation. The percentage reduction in binding of [$^3$H]-estradiol (Y) was calculated using the logit transformation of Y (logitY: ln[$y/1 − Y$]) versus the log of the mass of the competing steroid. The concentration of unlabeled steroid required to displace 50% of the bound [$^3$H]-estradiol was calculated for each steroid tested, and the results expressed as RBA. The RBA value of estradiol was by definition set equal to 100%.

**Computational Method for Computer Docking Experiments.** We compared the *cis*-6 non-covalent binding to the estrogen receptors with that of estradiol, and its known antagonist, ferrocifen, **3**.[1g,h,2,5] The guests, *cis*-6, **3**, and estradiol, were docked to the host, ER$\alpha$ or ER$\beta$, binding sites using ArgusLab 4.0.[12] Coordinates for the X-ray crystal structures of the ER$\alpha$ and ER$\beta$ estrogen receptors were taken from the Protein Databank (PDB).[13] We applied the ER$\alpha$ non-covalent interactions with estradiol (entry 1A52),[14] tamoxifen (entry **3ERD**),[15] and WAY-244 (entry **1X7E**),[10] as well as the ER$\beta$ non-covalent interactions with hydroxytamoxifen (entry **2FSZ**),[16] and WAY-244 (entry **1X78**).[10] The binding sites of the receptors were constructed based on the X-ray structures of the corresponding ligands. Both guest compound and receptor binding site geometries were flexibly set during docking. Docking simulations were performed using the Lamarckian Genetic Algorithm (GADock) docking engine. We found that the increase in population size, maximum generations, and local search maximum iterations resulted in generation of more stable conformations, in agreement with published results.[17] Thus, the population size was set to 100; test calculations with the population size increased to 200 did not improve the accuracy of the calculations. Similarly, we set maximum generations to 2000 and local search maximum iterations to 50. Default settings were used for other parameters of the calculations. The docking accuracy of such computational technique was expected to be close to that of rigorous commercial programs.[17] The geometry of *cis*-6 was taken from our previous rigorous DFT study,[6] which showed, in particular, that the complex was a dication in polar solutions. Thus, a formal 2+ charge was defined for the metal atom. Initial geometries of the other two guests were optimized at the same level of theory (PBE0/pc-1), see ref 6 for details of the previously reported DFT calculations.

(12) Thompson, M. A. *ArgusLab*, 4.0.1; Planaria Software LLC: Seattle, WA; http://www.arguslab.com.

(13) Berman, H. M.; Westbrook, J.; Feng, Z.; Gilliland, G.; Bhat, T. N.; Weissig, H.; Shindyalov, I. N.; Bourne, P. E. *Nucleic Acids Res.* **2000**, *28*, 235.

(14) Tanenbaum, D. M.; Wang, Y.; Williams, S. P.; Sigler, P. B. *Proc. Natl. Acad. Sci. U.S.A.* **1998**, *95*, 5998.

(15) Shiau, A. K.; Barstad, D.; Loria, P. M.; Cheng, L.; Kushner, P. J.; Agard, D. A.; Greene, G. L. *Cell* **1998**, *95*, 927.

(16) Wang, Y.; Chirgadze, N. Y.; Briggs, S. L.; Khan, S.; Jensen, E. V.; Burris, T. P. *Proc. Natl. Acad. Sci. U.S.A.* **2006**, *103*, 9908.

(17) Oda, A.; Okayasu, M.; Kamiyama, Y.; Yoshida, T.; Takahashi, O.; Matsuzaki, H. *Bull. Chem. Soc. Jpn.* **2007**, *80*, 1920.

**Supporting Information Available:** NOESY, COSY, HMBC, and HMQC correlation ^{1}H and ^{13}C NMR spectra for complex *trans*-**7** (7 pages), and a complete ref 10. This material is available free of charge via the Internet at http://pubs.acs.org.